

1 An updated synthesis of ocean total alkalinity and dissolved inorganic carbon measurements
2 from 1993 to 2023: the SNAPO-CO₂-v2 dataset

3
4 Nicolas Metzl¹, Jonathan Fin^{1,2,3}, Claire Lo Monaco¹, Claude Mignon¹, Samir Alliouane⁴, Bruno Bomblé⁵,
5 Jacqueline Boutin¹, Yann Bozec⁶, Steeve Comeau⁴, Pascal Conan^{7,8}, Laurent Coppola^{4,8}, Pascale Cuet⁹, Eva
6 Ferreira⁵, Jean-Pierre Gattuso^{4,10}, Frédéric Gazeau⁴, Catherine Goyet¹¹, Emilie Grossteffan¹², Bruno Lansard⁵,
7 Dominique Lefèvre¹³, Nathalie Lefèvre¹, Coraline Leseurre¹⁴, Sébastien Petton¹⁵, Mireille Pujo-Pay⁸, Christophe
8 Rabouille⁵, Gilles Reverdin¹, Céline Ridame¹, Peggy Rimmelin-Maury¹², Jean-François Ternon¹⁶, Franck
9 Touratier¹¹, Aline Tribollet¹, Thibaut Wagener¹³, Cathy Wimart-Rousseau¹⁷.

10
11¹ Laboratoire LOCEAN/IPSL, Sorbonne Université-CNRS-IRD-MNHN, Paris, 75005, France
12² OSU Ecce Terra, Sorbonne Université-CNRS, Paris, 75005, France

13³ Now at Institut des Sciences de la Terre, Grenoble, 38058, France

14⁴ Sorbonne Université, CNRS, Laboratoire d'Océanographie de Villefranche, LOV, F-06230 Villefranche-sur-
15 Mer, France

16⁵ Laboratoire des Sciences du Climat et de l'Environnement, LSCE/IPSL, UMR 8212 CEA- CNRS-UVSQ,
17 Université Paris-Saclay, 91191 Gif-sur-Yvette, France

18⁶ Station Biologique de Roscoff, UMR 7144 – EDYCO-CHIMAR, Roscoff, France

19⁷ Sorbonne Université, CNRS, Laboratoire d'Océanographie Microbienne, LOMIC, F-66650 Banyuls-sur-Mer,
20 France

21⁸ Sorbonne Université, CNRS OSU STAMAR - UAR2017, 4 Place Jussieu, 75252, Paris cedex 05, France

22⁹ Laboratoire ENTROPIE and Laboratoire d'Excellence CORAIL, Université de La Réunion-IRD- CNRS-
23 IFREMER-Université de la Nouvelle-Calédonie, 97744, Saint-Denis, La Réunion, France

24¹⁰ Institute for Sustainable Development and International Relations, Sciences Po, 27 rue Saint Guillaume, F-
25 75007 Paris, France

26¹¹ Espace-Dev UMR 228 Université de Perpignan Via Domitia, IRD, UM, UA, UG, 66860, Perpignan, France

27¹² Institut Universitaire Européen de la Mer (OSU-IUEM), Univ Brest, CNRS-UAR3113, 29280, Plouzané,
28 France

29¹³ Aix Marseille Univ, Université de Toulon, CNRS, IRD, MIO, Marseille, France

30¹⁴ Flanders Marine Institute (VLIZ), 8400 Ostend, Belgium

31¹⁵ Ifremer, Univ Brest, CNRS, IRD, LEMAR, F-29840 Argenton, France

32¹⁶ MARBEC, Univ Montpellier, CNRS, Ifremer, IRD, Sète, France

33¹⁷ National Oceanography Centre Southampton, European Way, Southampton, SO14 3ZH, UK

34
35 Correspondence to: Nicolas Metzl (nicolas.metzl@locean.ipsl.fr)

36
37 **Abstract.** Total alkalinity (A_T) and dissolved inorganic carbon (C_T) in the oceans are important properties to
38 understand the ocean carbon cycle and its link with global change (ocean carbon sinks and sources, ocean
39 acidification) and ultimately find carbon based solutions or mitigation procedures (marine carbon removal). We
40 present an extended database (SNAPO-CO₂, Metzl et al, 2024d) with 24700 new additional data for the period
41 2002 to 2023. The full database now includes more than 67000 A_T and C_T observations along with basic
42 ancillary data (time and space location, depth, temperature and salinity) in various oceanic regions obtained since
43 1993 mainly in the frame of French research projects. This includes both surface and water columns data
44 acquired in open oceans, coastal zones, rivers and in the Mediterranean Sea and either from time-series or
45 punctual cruises. Most A_T and C_T data in this synthesis were measured from discrete samples using the same
46 closed-cell potentiometric titration calibrated with Certified Reference Material, with an overall accuracy of ± 4
47 $\mu\text{mol kg}^{-1}$ for both A_T and C_T . The same technique was used onboard for underway measurements during cruises
48 conducted in the Southern Indian and Southern Oceans. The A_T and C_T data from these cruises are also added in

49 this synthesis. The data are provided in one dataset for the global ocean (<https://doi.org/10.17882/102337>) that
50 offers a direct use for regional or global purposes, e.g. A_T /Salinity relationships, long-term C_T estimates,
51 constraint and validation of diagnostics C_T and A_T reconstructed fields or ocean carbon and coupled
52 climate/carbon models simulations, as well as data derived from Biogeochemical-Argo (BGC-Argo) floats.
53 These data can also be used to calculate pH, fugacity of CO_2 ($f\text{CO}_2$) and other carbon system properties to derive
54 ocean acidification rates or air-sea CO_2 fluxes.

55

56 1 Introduction

57

58 The ocean plays a major role in reducing the impact of climate change by absorbing more than 90% of
59 the excess heat in the climate system (Cheng et al., 2020, 2024; von Schuckmann et al, 2023; IPCC, 2022) and
60 about 25% of human released CO_2 (Friedlingstein et al., 2022, 2023). In the last decade, the oceans experienced
61 a rapid warming, the year 2023 being the hottest since 1955 (Cheng et al, 2024). In the atmosphere the CO_2
62 concentration continues its terrific progressive rising, reaching 419.3 ppm in 2023 (a rate of +2.83 ppm yr⁻¹, Lan
63 et al 2024). In August 2024, the global atmospheric CO_2 concentration was already above 420 ppm. In the next
64 decade the oceans will continue to capture heat and CO_2 , somehow limiting the climate change, but this oceanic
65 CO_2 uptake changes the chemistry of seawater reducing its buffering capacity (Revelle and Suess, 1957; Jiang et
66 al, 2023). This process known as ocean acidification has potential impacts on marine organisms (Fabry et al.,
67 2008; Doney et al., 2009, 2020; Gattuso et al., 2015). With atmospheric CO_2 concentrations, surface ocean
68 temperature and ocean heat content, sea-level, sea-ice and glaciers, the ocean acidification (decrease of pH) is
69 now recognized by the World Meteorological Organization as one of the 7 key properties for global climate
70 indicators (WMO, 2018). Ocean acidification is specifically referred in the SDG indicator 14.3.1 coordinated at
71 the Intergovernmental Oceanographic Commission (IOC) of UNESCO. Observing the carbonate system in the
72 open oceans, coastal zones and marginal seas and understanding how this system changes over time is thus
73 highly relevant not only to quantify the global ocean carbon budget, the anthropogenic CO_2 inventories or ocean
74 acidification rates, but also to understand and simulate the processes that govern the complex CO_2 cycle in the
75 ocean (e.g. Goyet et al, 2016, 2019) and to better predict the future evolution of climate and global changes
76 (Eyring et al., 2016; Kwiatkowski et al., 2020; Jiang et al., 2023). As the rate of change in ocean acidification
77 presents large temporal and regional variability, long-term observations are required. Weekly to monthly regular
78 resolution data are needed to better investigate the long-term change of the carbonate system in regions subject
79 to extreme events (e.g. tropical cyclones, marine heat or cold waves, rapid freshening, convection, dust events,
80 river discharges, etc....). In this context it is recommended to progress in data synthesis of the ocean carbon
81 observations that would offer new high quality products for the community (e.g. for GOA-ON, www.goa-on.org,
82 IOC/SDG 14.1.3, <https://oa.iode.org/>, Tilbrook et al., 2019).

83 In this work, following the first SNAPO-CO₂ synthesis product (Metzl et al, 2024a), we present a new
84 synthesis of more than 67000 A_T and C_T data, measured either on shore or onboard Research Vessels obtained
85 over the 1993-2023 period during various cruises or at time-series stations mainly supported by French projects.
86 Hereafter this new dataset will be cited as SNAPO-CO₂-v2. The methods, data assemblage and quality control
87 were presented in version V1. Here, we describe the new data added and discuss some potential uses of this
88 dataset.

89

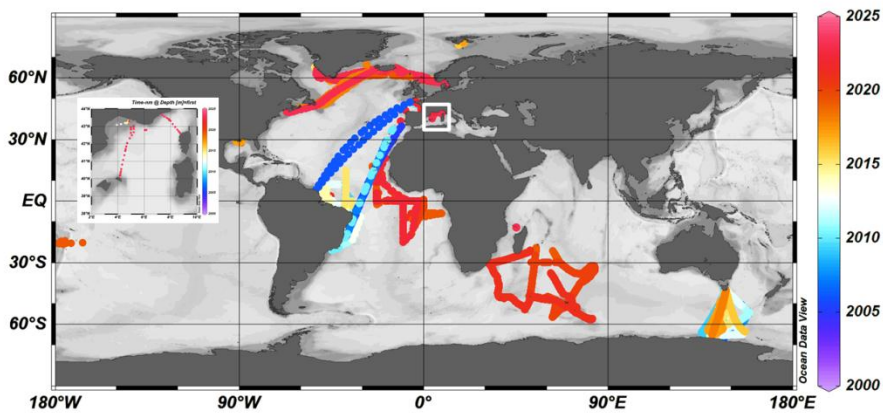
90 **2 Data collections**

91

92 The time series projects and research cruises from which new data were collated are listed in Table 1
 93 with information and references in the Supplementary file (Tables S1, S3 and S4). The sampling locations of
 94 new data are displayed in Figure 1 (the location for all data presented in Figure S1). Sampling was performed
 95 either from CTD-Rosette casts (Niskin bottles) or from the ship's seawater supply (intake at about 5m depth
 96 depending on the ship and swell). Samples collected in 500 mL borosilicate glass bottles were poisoned with 100
 97 to 300 μL of HgCl_2 depending on the cruises, closed with greased stoppers (Apiezon®) and held tight using
 98 elastic band following the SOP protocol (DOE, 1994; Dickson et al., 2007). Some samples were also collected in
 99 500 mL bottles closed with screw caps. After completion of each cruise, most of discrete samples were returned
 100 back to the LOCEAN laboratory (Paris, France) and stored in a dark room at 4 °C before analysis generally
 101 within 2-3 months after sampling (sometimes within a week). In this version we added data from samples that
 102 were also returned to University of Perpignan or to University of La Réunion. In addition to discrete samples
 103 analyzed for various projects conducted mainly in the North Atlantic, Tropical Atlantic, Mediterranean Sea and
 104 coastal regions (Table 1), we complemented this second synthesis with A_T and C_T surface observations obtained
 105 in the Indian and Southern oceans during the OISO cruises in 2019-2021 (Leseurre et al., 2022; Metzl et al,
 106 2022; data also available at NCEI/OCADS: www.nodc.noaa.gov/ocads/oceans/VOS_Program/OISO.html) and
 107 MINERVE cruises in 2002-2018 (Laika et al, 2009; Brandon et al, 2022). The A_T and C_T measurements from the
 108 MINERVE cruises were performed either onboard R/V Astrolabe or back in the laboratories (at LOCEAN
 109 laboratory and at University of Perpignan).

110

111



112

113

114

115

116

117

118

119

120

121 **Figure 1:** Locations of new A_T and C_T data (2005-2023) in the Global Ocean and the Western Mediterranean Sea
 122 (white box, insert) in the SNAPO-CO₂-v2 dataset. Color code is for Year. Figure produced with ODV (Schlitzer,
 123 2018).

124

125 **Table 1:** List of cruises added in the SNAPO-CO₂-v2 dataset. This is organized by region from North to South
 126 and the Mediterranean Sea. See Tables S1, S2, S3 and S4 in the Supplementary Material for a list of laboratories,
 127 of CRMs used, for DOI and for references of cruises. Nb = the number of data for each cruise or time-series. *
 128 indicates the measurements at sea (surface underway).

Cruise/Project	Start	End	Region	Sampling	Nb
STEP	2016	2017	Arctic	Water Column	33
SURATLANT AX1	2017	2023	North Atlantic	Surface	255
SURATLANT AX2	2018	2023	North Atlantic	Surface	224
VOS	2005	2010	Atlantic	Surface	192
MISSRHODIA-1	2017	2017	Gulf Mexico	Water Column	8
ACIDHYPO	2022	2022	Gulf Mexico	Water Column	10
CAMFIN-WATL	2010	2015	Trop Atlantic	Surface	192
PIRATA-BR	2009	2015	Trop Atlantic	Surface	194
BIOAMAZON	2013	2014	Trop Atlantic	Surface	62
AMAZOMIX	2021	2021	Trop Atlantic	Water Column	180
PIRATA-FR	2019	2019	Trop Atlantic	Surface	93
PIRATA-FR	2020	2020	Trop Atlantic	Surface, Water Column	58
PIRATA-FR	2021	2021	Trop Atlantic	Surface, Water Column	79
PIRATA-FR	2022	2022	Trop Atlantic	Surface, Water Column	118
CO2ARVOR	2009	2010	Atlantic, Coastal	Surface, Water Column	621
SOMLIT-Roscoff	2020	2022	Coastal North Atl	Surface and 60m	207
SOMLIT-Brest	2020	2022	Coastal North Atl	Surface	251
TONGA	2019	2019	Trop Pacific	Water Column	226
CARBODISS	2018	2019	Indian Mayotte	Surface	85
OISO *	2019	2021	South Indian	Surface	5258
MINERVE	2004	2018	Southern Ocean	Surface	1077
MINERVE *	2002	2013	Southern Ocean	Surface	11258
COCORICO2	2017	2022	Coastal	Surface	589
SOMLIT-PointB	2019	2023	MedSea Coastal	Surface and 50m	716
SOLEMIO	2018	2022	MedSea Coastal	Water Column	271
ANTARES	2017	2023	MedSea	Water Column	506
MOLA	2018	2023	MedSea Coastal	Water Column	193
DYFAMED	2018	2023	MedSea	Water Column	514
MESURHO-BENT	2010	2011	MedSea Coastal	Surface and sub-surface	25
ACCESS-01	2012	2012	MedSea Coastal	Water Column	16
CARBO-DELTA-2	2013	2013	MedSea Coastal	Water Column	14
DICASE	2014	2014	MedSea Coastal	Water Column	22
MISSRHODIA-2	2018	2018	MedSea Coastal	Surface and sub-surface	13
DELTARHONE1	2022	2022	MedSea Coastal	Water Column	9
MOOSE-GE	2021	2021	MedSea	Water Column	451
MOOSE-GE	2022	2022	MedSea	Water Column	447
MOOSE-GE	2023	2023	MedSea	Water Column	475

173 3 Method, accuracy, repeatability and quality control

175 3.1 Method and accuracy

177 Since 2003, the discrete samples returned back at SNAPO-CO₂ Service facilities (LOCEAN, Paris),
 178 were analyzed simultaneously for A_T and C_T by potentiometric titration using a closed cell (Edmond, 1970;
 179 Goyet et al., 1991). The same technique was used at sea for surface water underway measurements during OISO
 180 and MINERVE cruises (indicated by * in Table 1). In the late 1980s the so-called “JGOFS-IOC Advisory Panel
 181 on Ocean CO₂” recommended the need for standard analysis protocols and for developing Certified Reference
 182 Materials (CRMs) for inorganic carbon measurements (Poisson et al., 1990; UNESCO, 1990, 1991). The CRMs

were provided to international laboratories by Pr. A. Dickson (Scripps Institution of Oceanography, San Diego, USA), starting in 1990 for C_T and 1996 for A_T , respectively. These CRMs were thus always available to us and used to calibrate the measurements (CRM Batch numbers used for each cruise are listed in the Supplementary file, Table S2). The CRMs accuracy, as indicated in the certificate for each Batch, is around $\pm 0.5 \mu\text{mol kg}^{-1}$ for both A_T and C_T (www.nodc.noaa.gov/ocads/oceans/Dickson_CRM/batches.html). The concentrations of CRMs we used vary between 2193 and 2426 $\mu\text{mol kg}^{-1}$ for A_T and between 1968 and 2115 $\mu\text{mol kg}^{-1}$ for C_T corresponding to the range of concentrations observed in open ocean water. In the Mediterranean Sea the concentrations are higher ($A_T > 2600 \mu\text{mol kg}^{-1}$ and $C_T > 2300 \mu\text{mol kg}^{-1}$) and in the coastal zones or near the Amazon River plume the concentrations were often lower than the CRMs ($A_T < 1500 \mu\text{mol kg}^{-1}$ and $C_T < 1000 \mu\text{mol kg}^{-1}$). Results of analyses performed on 1242 CRM bottles (different Batches) in 2013-2024 are presented in Figure 2. The standard-deviations (Std) of the differences of measurements were on average $\pm 2.69 \mu\text{mol kg}^{-1}$ for A_T and $\pm 2.88 \mu\text{mol kg}^{-1}$ for C_T . For unknown reasons, the differences were occasionally up to 10-15 $\mu\text{mol kg}^{-1}$ (1.2% of the data, Figure S2). These few CRM measurements were discarded for the data processing. We did not detect any specific signal for CRM analyses (e.g., larger uncertainty depending on the Batch number or temporal drifts during analyses, Figure 2) but for some cruises the accuracy based on CRMs could be better than 3 $\mu\text{mol kg}^{-1}$ (e.g. $< 3 \mu\text{mol kg}^{-1}$ for AMAZOMIX cruise using 6 Batches #197 and for MOOSE-GE 2022 using 19 Batches #204, or $< 1.5 \mu\text{mol kg}^{-1}$ for SOMLIT-Point-B in 2022 using 6 Batches #204).

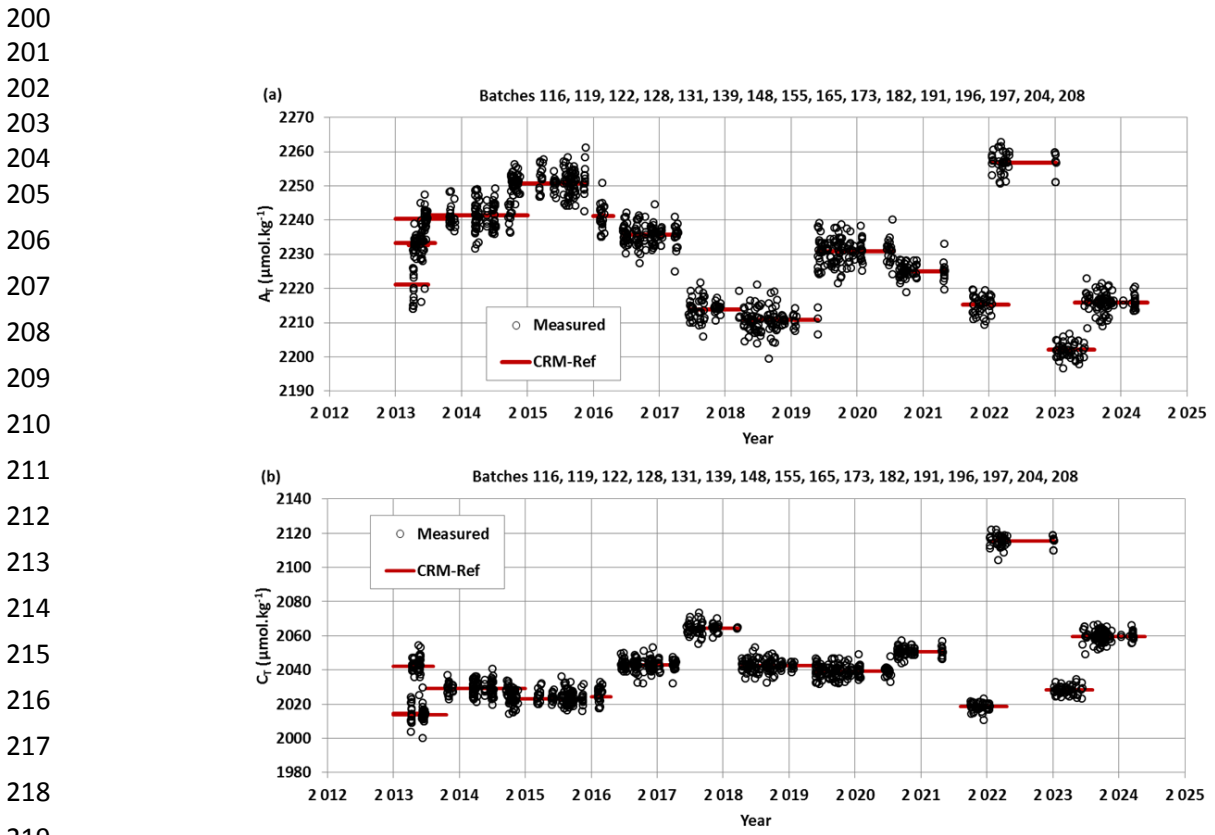
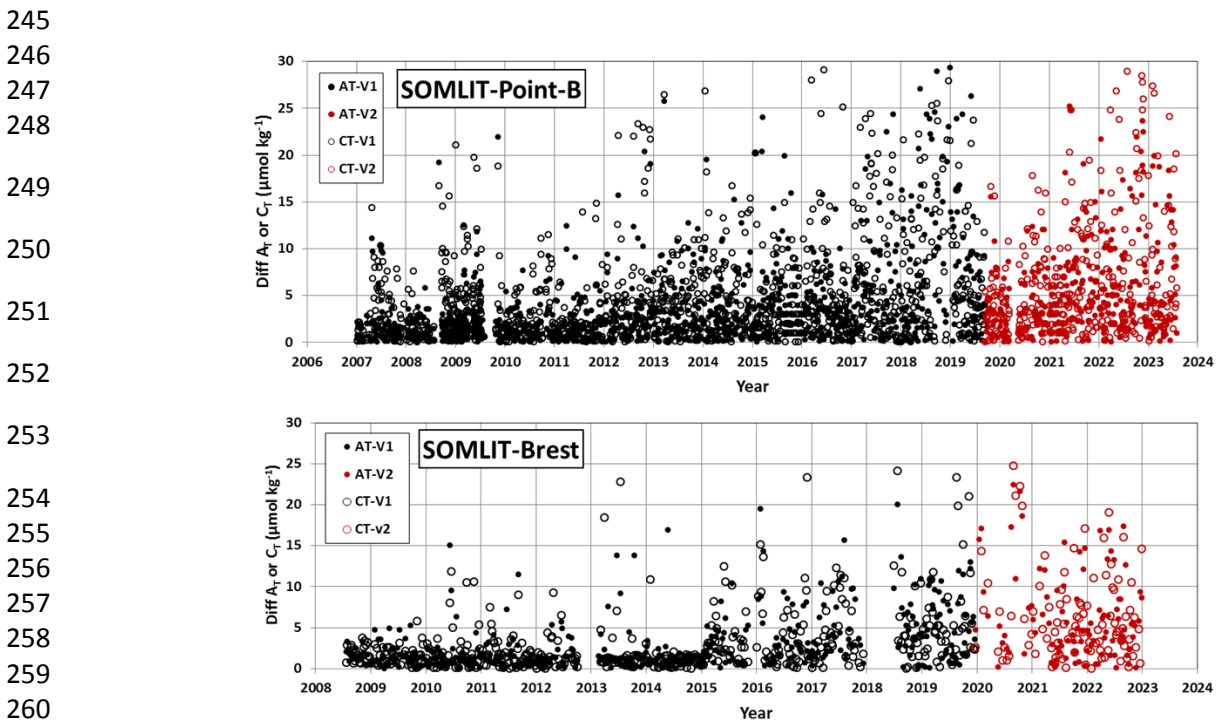


Figure 2: A_T (a) and C_T (b) analyses for different CRM Batches measured in 2013-2024. For these 1242 analyses the mean and standard-deviations of the differences with the CRM reference were $-0.11 (\pm 2.69) \mu\text{mol kg}^{-1}$ for A_T and $0.01 (\pm 2.88) \mu\text{mol kg}^{-1}$ for C_T .

226 **3.2 Repeatability**
 227

228 For some projects, duplicates have been regularly sampled (SOMLIT-Point-B, SOMLIT-Brest) or
 229 replicate bottles sampled at selected depths at fixed stations during the cruises (e.g. STEP, CARBODISS). In the
 230 first synthesis of the SNAPO-CO₂ dataset we showed the results from several time-series (SOMLIT-Point-B,
 231 SOMLIT-Brest and BOUSSOLE/DYFAMED). Here we present the results for the new data obtained at
 232 SOMLIT-Point-B in the coastal Mediterranean Sea and SOMLIT-Brest in the Bay of Brest (Figure 3). Results of
 233 A_T and C_T repeatability are synthetized in Table 2. For the OISO cruises conducted in 2019, 2020 and 2021 the
 234 repeatability was evaluated from duplicate analyses (within 20 minutes time) of continuous sea surface
 235 underway sampling at the same location (when the ship was stopped). Similarly to what was found for the CRM
 236 measurements (Figure S2), differences in duplicates are occasionally higher than 10-15 $\mu\text{mol kg}^{-1}$ (Figure 3) but
 237 most of the duplicates for all projects are within 0 to 3 $\mu\text{mol kg}^{-1}$. Compared to previous results (Kapsenberg et
 238 al. 2017; Metzl et al. 2024a), there are larger differences between duplicates at SOMLIT-B in 2019-2023 (up to
 239 30 $\mu\text{mol kg}^{-1}$, Figure 3) leading to relatively large Std around 5 and 6 $\mu\text{mol kg}^{-1}$ for both A_T and C_T (Table 2).
 240 The same was observed for duplicates at SOMLIT-Brest (Table 2). We do have not yet a clear explanation for
 241 this large Std although larger variability was observed in recent years, and the measurements were performed
 242 later after the sampling (e.g. more than 6 months for some samples during and after the COVID period). We will
 243 see that given the temporal variability of the properties this does not lead to suspicious interpretation for the
 244 seasonality or the trend analyses of these time-series.



263 **Figure 3:** Results of duplicate A_T and C_T analyses from the time-series SOMLIT-Point-B in the coastal
 264 Mediterranean Sea and SOMLIT-Brest in the coastal Brittany for the data in the SNAPO-CO₂-v1 dataset (black)
 265 and new data added in SNAPO-CO₂-v2 (red). The plots show differences in duplicates for both A_T (filled
 266 circles) and C_T (open circles). Standard-deviations of these duplicates are listed in Table 2.
 267
 268

269 **Table 2:** Repeatability of A_T and C_T analyses for cruises with duplicate analysis. The results are expressed as the
 270 standard-deviations (Std) of the analysis of replicated samples. Nb = the number of replicates for each Time-
 271 series or Cruise. For the OISO cruises the mean repeatability was obtained from measurements at the same
 272 location (when the ship stopped).

Cruise	Period	Nb	Std A_T $\mu\text{mol kg}^{-1}$	Std C_T $\mu\text{mol kg}^{-1}$	Reference
STEP	2017	3	0.7	2.8	Unpublished
CARBODISS	2018	10	6.72	5.71	Unpublished
SOMLIT-Point-B	2007-2019	1130	4.5	5.1	SNAPO-CO2-v1, (a)
SOMLIT-Point-B	2019-2023	321	5.2	6.2	SNAPO-CO2-v2, (a)
SOMLIT-Brest	2008-2018	404	3.1	3.4	SNAPO-CO2-v1, (a)
SOMLIT-Brest	2019-2022	142	6.0	6.1	SNAPO-CO2-v2, (a)
OISO 29	2019	46	1.8	1.8	Leseurre et al (2022), (b)
OISO 30	2020	67	1.5	2.0	Metzl et al. (2022), (b)
OISO 31	2021	343	2.6	3.3	Metzl et al (2024c), (b)

292 (a) See Figure 3 for the results of regular duplicates for time-series SOMLIT-Point-B, SOMLIT-Brest.

293 (b) Metadata and data available at www.nodc.noaa.gov/ocads/oceans/VOS_Program/OISO.html

295 3.3 Assigned flags for quality control

297 Identifying each data with an appropriate flag is very convenient for selecting the data (good,
 298 questionable or bad). Here we used 4 flags for each property (flags 2 = good, 3= questionable, 4=bad, and 9= no
 299 data) following the WOCE program and used in other data products such as SOCAT (Bakker et al., 2016) or
 300 GLODAP (Olsen et al., 2016; Lauvset et al., 2024). During the data-processing, we first assigned a flag for each
 301 A_T and C_T data based on the standard error in the calculation of A_T and C_T concentrations (non-linear regression,
 302 Dickson et al. 2007). By default, if the standard deviation on the regression is $> 1 \mu\text{mol kg}^{-1}$, we assigned a flag 3
 303 (questionable) although the data could be acceptable and then used for interpretations. Flag 3 was also assigned
 304 when salinity was doubtful or when differences of duplicates were large (e.g. $\pm 20 \mu\text{mol kg}^{-1}$). Flags 4 (bad or
 305 certainly bad) were assigned when clear anomalies were detected for unknown reasons (e.g. a sample probably
 306 not fixed with HgCl_2 or analysis performed late during the COVID issue). A secondary quality control was
 307 performed by the PIs of each project based on data inspection, duplicates, A_T /Salinity relationship, or the mean
 308 observations in deep layers where large variability in A_T and C_T is unlikely to occur from year to year.

309 An example for quality flag is presented for all data from the MINERVE cruises conducted in 2002-
 310 2018 in the Southern Ocean where clear outliers have been identified (Figure S3). For the MINERVE cruises in
 311 2002-2018 and a total of 12335 A_T and C_T analyses, 24 were identified as bad (flag 4), 978 for A_T and 971 for C_T
 312 listed as questionable (flag 3), and all others are considered as good data (flag 2, i.e. about 92%). For the
 313 MOOSE-GE cruises in 2021, 2022 and 2023 (new data in SNAPO-CO2-v2) and a total of 1373 A_T and C_T
 314 analyses, 2 were identified flagged as bad (flag 4), 38 for A_T and 33 for C_T listed as questionable (flag 3) all
 315 others were considered as good data (flag 2, i.e. 97%). This is better than the statistics we evaluated for the
 316 SNAPO-CO2-v1 dataset (90% flag 2 for MOOSE-GE in 2010-2019). A similar control was performed for each
 317 project.

318 **3.4 Inter-comparisons**

319

320 Inter-comparisons of measurements performed for different cruises or with different techniques help to
321 evaluate the quality of the data and detect potential biases when merging the data in the same region obtained by
322 different laboratories at different periods. This is especially important to interpret long-term trends of A_T and C_T
323 as well as for $p\text{CO}_2$ and pH calculated with A_T C_T pairs. The synthesis of various cruises in the same region and
324 periods also offers verification and secondary control of the data.

325

326 **3.4.1 Comparisons in deep layers**

327

328 Comparisons of data in the deep layers from different cruises are useful for secondary quality control as
329 one expects low natural variability or anthropogenic signals from season to season and over a few years. Several
330 cruises were conducted in the Mediterranean Sea in 2017-2023 (MOOSE-GE, ANTARES and DYFAMED). The
331 mean values of C_T and A_T in the deep layers ($> 1800\text{m}$) for each cruise confirmed the coherence of the data
332 (Table 4). The C_T and A_T concentrations are also in the range of the mean values evaluated for cruises conducted
333 in 2014 in the Mediterranean Sea (results listed in the SNAPO-CO₂-v1 synthesis, Metzl et al., 2024a). In the
334 western tropical Pacific we also observed coherent properties for the TONGA and OUTPACE cruises (Wagener
335 et al., 2018) for data selected at 1800-2300m layer corresponding to the C_T maximum layer in the Pacific Deep
336 Water (PDW). On the other hand in the western tropical Atlantic near the Amazon River plume where the spatial
337 variability of the properties is large at the surface (Ternon et al., 2000; Mu et al., 2021; Olivier et al., 2022) the
338 comparison in the water column is less clear (Figure S4). Nevertheless for the AMAZOMIX and the TARA-
339 Microbiome cruises, both conducted in September 2021, the results at close stations (around 5°N/50°W) suggest
340 very similar concentrations at 1000m (Table 4). The comparisons in deep waters enabled to merge the different
341 datasets for interpretations of the temporal trends and processes driving the CO₂ cycle in these regions (e. g.
342 Ulles et al., 2023 and Wimart-Rousseau et al., 2023 for the Mediterranean Sea)

343

344 **3.4.2 Comparing on board and on shore results**

345

346 In surface waters where the variability is high inter-comparison is not relevant for secondary quality
347 control. However, during the MINERVE cruises, discrete samples were occasionally performed along with sea
348 surface underway measurements. Thus, we can compare A_T and C_T measured in the laboratory with those
349 measured onboard as described by Laika et al. (2009) for the MINERVE cruises in 2005-2006. It should be
350 noticed that the discrete samples were measured after a long trip (shipping boxes from Hobart, Tasmania to
351 Paris, France) and thus generally analyzed at least 3 months after the cruises (cruises conducted in October to
352 February, analyses performed in May-June). Given all the uncertainties associated to the sampling, samples
353 storage and transport, analyses and CRMs, the mean differences between discrete and underway data are still
354 reasonable (Std ranging between 4 and 12 $\mu\text{mol kg}^{-1}$, Table 5). For unknown reasons the mean difference was
355 high for a cruise in 2008-2009 (Std $> 10 \mu\text{mol kg}^{-1}$, the “weather goal”, Newton et al., 2015). With this in mind,
356 we believe the MINERVE data (both underway and discrete data) are useful to interpret the change of properties
357 in this region at seasonal or decadal scales (Laika et al., 2009; Brandon et al., 2022).

358

359 **Table 4:** Mean observations in the deep layers ($> 1800\text{m}$) of the Ligurian Sea (Western Mediterranean Sea for
 360 different cruises conducted in 2017-2023), of the Tropical Pacific (around 2000m for cruises in 2017 and 2019),
 361 and of the Tropical Atlantic (around 1000m for cruises in 2021). N- A_T and N- C_T are A_T and C_T normalized at
 362 salinity (S = 38 in the Ligurian Sea; S= 35 for the Pacific and the Atlantic Oceans). Nb = number of data (with
 363 flag 2). Standard deviations are in brackets.

Cruise	Period	Nb	Pot. Temp (°C)	Salinity	N- A_T ($\mu\text{mol kg}^{-1}$)	N- C_T ($\mu\text{mol kg}^{-1}$)
Ligurian Sea ($> 1800\text{m}$)						
All Cruises	2017-2023	227	12.923 (0.052)	38.484 (0.003)	2558.3 (10.5)	2300.0 (10.7)
DYFAMED	2017-2022	74	12.913 (0.006)	38.485 (0.002)	2555.1 (11.8)	2297.3 (12.4)
ANTARES	2017-2023	62	12.944 (0.096)	38.485 (0.005)	2559.8 (9.0)	2302.2 (8.9)
MOOSE-GE	2017-2023	91	12.917 (0.005)	38.484 (0.003)	2559.8 (9.8)	2300.7 (10.0)
Tropical Pacific (layer 1800-2300m)						
OUTPACE	2017	15	2.124 (0.055)	34.633 (0.006)	2414.1 (8.0)	2318.8 (5.8)
TONGA	2019	7	2.196 (0.197)	34.619 (0.016)	2408.9 (9.1)	2327.2 (7.5)
Western Tropical Atlantic (1000m)						
AMAZOMIX	2021	14	4.770 (0.105)	34.711 (0.041)	2315.6 (20.2)	2220.8 (17.1)
TARA-MICRO	2021	1	4.852	34.717	2312.9	2231.1

402 **Table 5:** Comparison of A_T and C_T analysed on-board and at SNAPO-CO₂ facilities for the MINERVE project.
 403 The results are expressed as the standard deviations (Std) of the differences for each cruise. Nb = the number of
 404 co-located samples.

Period	Nb	Std A_T $\mu\text{mol kg}^{-1}$	Std C_T $\mu\text{mol kg}^{-1}$
2004-2005	109	12.85	4.99
2005-2006	45	4.20	6.77
2007-2008	17	10.15	10.62
2008-2009	26	15.80	12.02
2009-2010	22	4.04	5.78
2010-2011	33	9.36	6.83
2012-2013	29	5.43	9.73

421 **3.4.3 Comparison based on different techniques**

422

423 Another example of comparison is presented for samples obtained in the lagoon of Mayotte Island in
 424 the western Indian Ocean and measured using different techniques. In the frame of the CARBODISS project
 425 seawater was sampled in 2018-2023 at several coral reef sites within the north-eastern part of the lagoon and
 426 measured either at LOCEAN laboratory or at La Réunion University. To remove coral sand particles the water
 427 samples were immediately filtered through Whatman GF/F filters and poisoned with mercuric chloride,
 428 following Dickson et al. (2007). In 2021, 2022 and 2023, A_T was measured at La Réunion University using an
 429 automated potentiometric titration (905 Titrando Metrohm titrator with combined pH electrode 6.0253.00) and
 430 calculated from the second inflection point of the titration curve. The HCl concentration was checked each day
 431 of measurements using a CRM provided by A. Dickson, Scripps Institution of Oceanography. The A_T precision
 432 of $\pm 2 \mu\text{mol kg}^{-1}$ was based on triplicate analyses (Lagoutte et al., 2023). In the studied coral reef sites A_T
 433 concentrations ranged between 2250 and 2350 $\mu\text{mol kg}^{-1}$ but with occasional higher concentrations up to 2450-
 434 2500 $\mu\text{mol kg}^{-1}$. Such high A_T has been observed in other coral reefs ecosystems (Cyronek et al., 2013 at Cook
 435 Island; Palacio-Castro et al., 2023 at Middle Keys, Florida). The data obtained in the lagoon of Mayotte on
 436 different coral reefs could be compared with underway observations obtained offshore of Mayotte Island (OISO-
 437 11 cruises in 2004 and CLIM-EPARSES cruise in 2019, data available in the SNAPO-CO2-v1 dataset). In the
 438 open ocean the A_T concentrations ranged between 2250 and 2330 $\mu\text{mol kg}^{-1}$, close to the results obtained at
 439 Mayotte reefs except for samples in November 2021 that were all collected at Cratère station (12.84°S-45.39°E)
 440 (Figure 4). At this location there was a large diurnal variation in November 2021 with A_T increasing from 2322
 441 to 2508 $\mu\text{mol kg}^{-1}$ (Figure S5). This is because in 2021 the samples were taken at low tide recording a volcanic
 442 signal at this site allowing recording for the first time the volcanic signal in this location (CO₂ resurgences). In
 443 2018 and 2019 such high A_T were not measured (Figure S5) as samples were taken at high tides allowing a
 444 certain dilution of volcanic CO₂ emissions in the water column. Although the samples were measured with
 445 different techniques the range of A_T is coherent for both datasets (Figure 4). Therefore we added the A_T data
 446 measured at La Réunion University in 2021-2023 to complete the synthesis for this location (Mayotte Island).

447

448

449

450

451

452

453

454

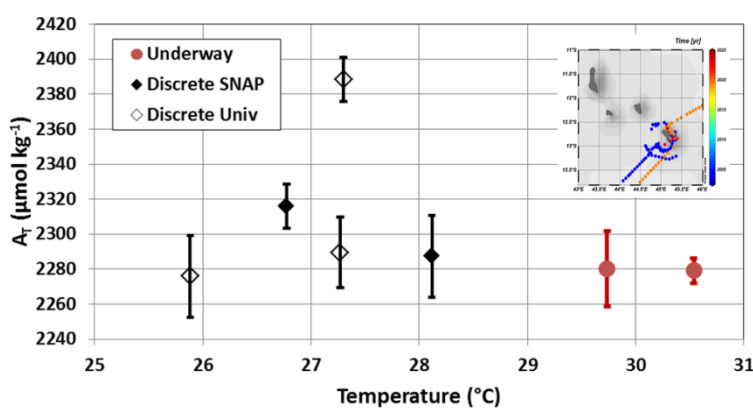
455

456

457

458

459



460 **Figure 4:** Total alkalinity (A_T) versus temperature for samples measured around Mayotte and in the coral reef
 461 (insert map). Underway A_T was measured onboard in 2004 and 2019 (red circles) whereas discrete samples at
 462 different reef sites within the lagoon of Mayotte in 2018, 2019, 2021, 2022 and 2023 were measured at
 463 LOCEAN (black diamonds) or at La Réunion University (open diamonds). The figure presents the data averaged
 464 for each cruise in this region.

465

466 **3.4.4 Summary of quality control data**

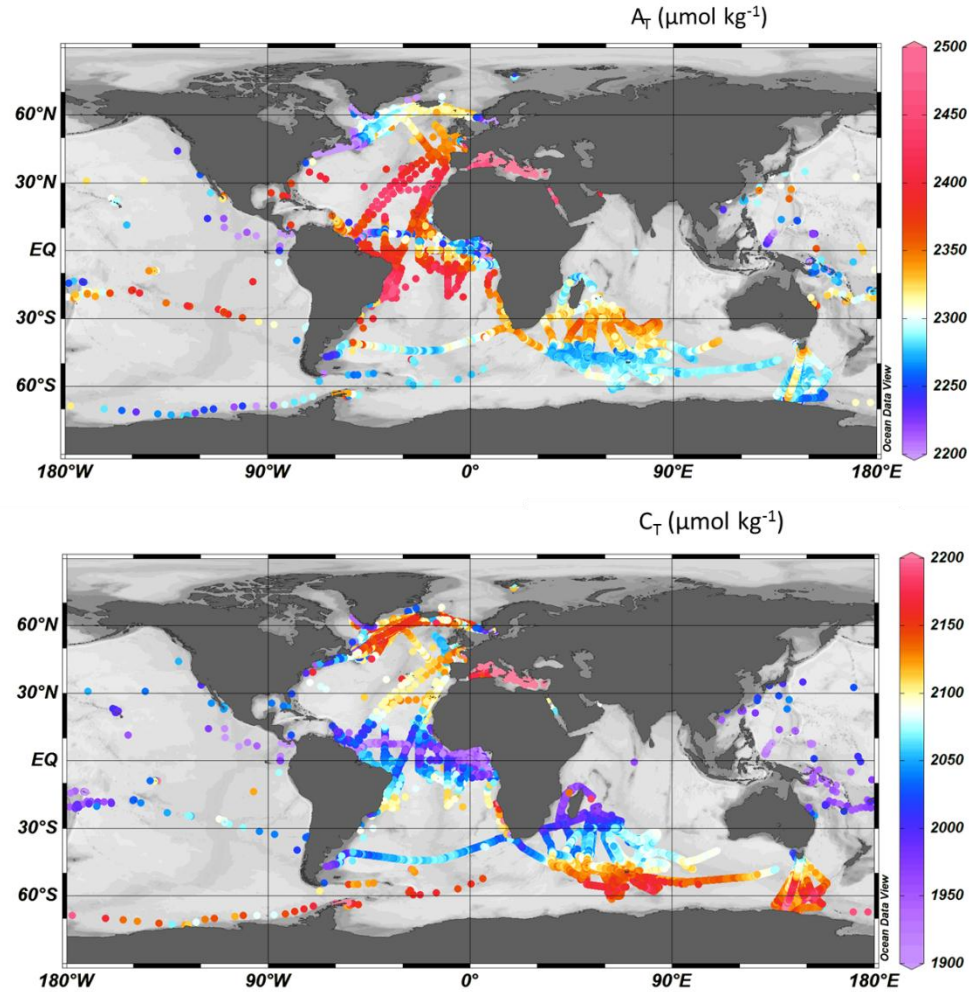
467
468 The total number of data in the SNAPO-CO2-v2 dataset for the Global Ocean is gathered in Table 6
469 with corresponding flags for each property. Overall, the synthesis includes more than 91% of good data for both
470 A_T and C_T . About 6% are questionable and 3% are likely bad. Overall, we believe that all data (with flag 2) in
471 this synthesis have an accuracy better than 4 $\mu\text{mol kg}^{-1}$ for both A_T and C_T , the same as for quality-controlled
472 data in GLODAP (Lauvset et al., 2024). The uncertainty ranges between the “Climate goal” (2 $\mu\text{mol kg}^{-1}$) and
473 the “Weather Goal” (10 $\mu\text{mol kg}^{-1}$) for ocean acidification studies (Newton et al., 2015; Tilbrook et al., 2019).
474 This accuracy is also relevant to validate or constraint data-based methods that reconstruct A_T and C_T fields with
475 an error of around 10-15 $\mu\text{mol kg}^{-1}$ for both properties (Bittig et al., 2018; Broullón et al., 2019, 2020; Fourrier et
476 al., 2020; Gregor and Gruber, 2021; Chau et al., 2024a).

477
478
479 **Table 6:** Number of Temperature, Salinity, A_T and C_T data in the SNAPO-CO2-v2 synthesis identified for flags
480 2 (good), 3 (questionable), 4 (bad), 9 (no data). Last column is the percentage of flag 2 (Good).

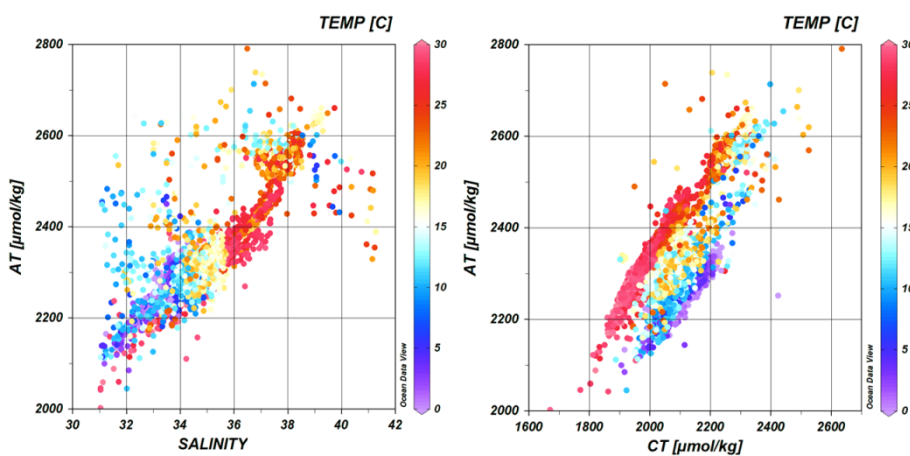
Property	Flag 2	Flag 3	Flag 4	Flag 9	% flag 2
Temperature	68253	418	0	653	99.4
Salinity	68706	482	5	131	99.3
A_T	61249	3910	2077	2088	91.1
C_T	61869	3865	2057	1533	91.3

492 **4 Global A_T and C_T distribution based on the SNAPO-CO2-v2 dataset**

493
494 The surface distribution in the global ocean based on the SNAPO-CO2 dataset is presented in Figure 5
495 for A_T and C_T . The A_T /Salinity and A_T/C_T relationships are clearly identified and structured at regional scale
496 (Figure 6). In the open ocean, high A_T concentrations ($> 2400 \mu\text{mol kg}^{-1}$) are identified in the Atlantic subtropics
497 (bands 35°N-15°N and 25°S-3°S) (Jiang et al., 2014; Takahashi et al., 2014). The lowest A_T and C_T
498 concentrations ($< 600 \mu\text{mol kg}^{-1}$) are observed in the western tropical Atlantic in the Amazon River plume near
499 the mouth (Lefèvre et al., 2017b). For C_T the concentrations are high ($> 2150 \mu\text{mol kg}^{-1}$) in the Southern Ocean
500 south of the polar front, associated with the deep mixing in winter and the upwelling of deep water (Metzl et al.,
501 2006; Pardo et al., 2017). The highest C_T concentrations (up to 2180-2270 $\mu\text{mol kg}^{-1}$) are observed in the high
502 latitudes of the Southern Ocean near the Adélie coastal zone (MINERVE and ACE cruises), around the
503 Kerguelen plateau (OISO-31 cruise) and close to the Antarctic Peninsula (TARA-Microbiome cruise). In the
504 North Atlantic the new data from SURATLANT cruises in 2018-2023 confirm the high C_T concentrations ($>$
505 2150 $\mu\text{mol kg}^{-1}$) observed in the Sub-polar gyre since 2016 due in part to the accumulation of anthropogenic CO₂
506 (Leseurre et al., 2020). Low C_T concentration ($< 2000 \mu\text{mol kg}^{-1}$) are found in the tropics (10°N-30°S) with
507 lower values ($< 1950 \mu\text{mol kg}^{-1}$) in the equatorial Atlantic band 10°N-Eq (e.g. Koffi et al., 2010; Lefèvre et al.,
508 2021). In the Amazon shelf sector C_T can reach even lower concentration ($< 1700 \mu\text{mol kg}^{-1}$, AMAZOMIX
509 cruise).



539 **Figure 5:** Distribution of A_T (top) and C_T (bottom) concentrations ($\mu\text{mol.kg}^{-1}$) in surface waters (0-10m) in the
540 SNAPO-CO₂-v2 dataset. Only data with flag 2 are presented in these figures. Figures produced with ODV
541 (Schlitzer, 2018).



560 **Figure 6:** Relationships between A_T and Salinity (left panel) and A_T versus C_T (right panel) for samples in
561 surface waters (0-10m and Salinity > 31). Only data with flag 2 are presented (nb = 48749). The color scales
562 correspond to the temperature. The data not aligned correspond to coastal zones (e.g. COCORICO₂ stations).
563 Figures produced with ODV (Schlitzer, 2018).

564

565 **5 Regional A_T and C_T distributions and trends based on the SNAPO-CO₂ dataset**

566

567 The regional distributions are described for the Mediterranean Sea and for selected regions in the open
 568 ocean and coastal zones where the data are available for 10 years or more to explore the A_T and C_T trends. Given
 569 the observed seasonal and inter-annual variability and that the time-series were not regular (e.g. at monthly
 570 frequency), we cannot use recommended methods to estimate the trends (e.g. based on de-seasoned data, Sutton
 571 et al., 2022). Here we have selected the locations and seasons where the C_T trends can be linearly fitted and
 572 compared with no interpolation to fill gaps and discontinuous data (e.g., fewer samples during the COVID
 573 period).

574

575 **5.1 The Mediterranean Sea**

576

577 Compared to the open ocean, A_T concentrations are much higher in the Mediterranean Sea (Copin-
 578 Montégut, 1993; Schneider et al., 2007; Álvarez et al., 2023) with values up to 2600 $\mu\text{mol kg}^{-1}$. The A_T and C_T
 579 data obtained in 2014-2023 show a clear contrast between the northern and southern regions of the Western
 580 Mediterranean Sea with higher concentration in the Ligurian Sea and the Gulf of Lion (Figure 7). This contrast is
 581 associated to the circulation and the frontal system in this region (e.g. Barral et al., 2021). New data in the coastal
 582 zones in the Gulf of Lion (ACCESS, DICASE, CARBODELTA, COCORICO₂, MESURHOBENT) also have
 583 very high A_T and C_T concentrations ($A_T > 2600 \mu\text{mol kg}^{-1}$; $C_T > 2350 \mu\text{mol kg}^{-1}$). Very low A_T and C_T
 584 concentrations ($A_T < 2500 \mu\text{mol kg}^{-1}$; $C_T < 2200 \mu\text{mol kg}^{-1}$) were also occasionally observed in the coastal zones
 585 (COCORICO₂ stations, Petton et al., 2024).

586 In summer 2022 the Mediterranean Sea experienced an exceptional warming (Figure S6) superposed to
 587 the long-term warming in the ocean (Cheng et al., 2024). Such event would impact the internal ocean processes
 588 such as thermodynamic, stratification and biological processes (Coppola et al., 2023) and the inter-annual
 589 variability and trends of C_T , pH, $f\text{CO}_2$ and air-sea CO_2 fluxes (Yao et al., 2016; Wimart-Rousseau et al., 2023;
 590 Chau et al., 2024b). As in 2003, the warming in summer 2022 was associated to the drought event that occurred
 591 in Europe and over the Mediterranean Sea (Faranda et al., 2023). In July 2022, the maximum temperature of
 592 28.42°C was observed at station SOMLIT-Point-B. In the Ligurian Sea the temperature trend was faster in recent
 593 years, $+0.173 \pm 0.072^\circ\text{C}$ per decade over 1990-2010 and $+0.678 \pm 0.143$ per decade over 2010-2023 (Figure
 594 S6). With the new data added in the SNAPO-CO₂-v2 synthesis (DYFAMED, MOOSE-ANTARES, and
 595 MOOSE-GE) we evaluated a temperature trend of $+0.84 \pm 0.20^\circ\text{C}$ per decade over 1998-2022 indicating that
 596 the discrete sampling captured the property changes at regional scale. Based on the data in the Ligurian Sea the
 597 trends of C_T appeared faster in summer ($+1.53 \pm 0.46 \mu\text{mol kg}^{-1} \text{yr}^{-1}$) than in winter ($+0.94 \pm 0.64 \mu\text{mol kg}^{-1} \text{yr}^{-1}$,
 598 Table 7). On the other hand, the trends of A_T were the same ($+0.72 \pm 0.36 \mu\text{mol kg}^{-1} \text{yr}^{-1}$ in winter and $+0.69 \pm$
 599 $0.42 \mu\text{mol kg}^{-1} \text{yr}^{-1}$ in summer). The trend of C_T in surface in winter was close to the one derived at 100m (below
 600 the Chl-a maximum), $C_T^{100\text{m}} = +1.10 \pm 0.17 \mu\text{mol kg}^{-1} \text{yr}^{-1}$ (Figure 8) whereas for A_T the trend was the same in
 601 surface and at depth ($+0.76 \pm 0.12 \mu\text{mol kg}^{-1} \text{yr}^{-1}$). This suggests that the winter C_T data recorded the
 602 anthropogenic CO_2 uptake of around $+1 \mu\text{mol kg}^{-1} \text{yr}^{-1}$, Figure S7). Note that, given the observed C_T trends, the
 603 spatial view presented in Figure 7b for 2014-2023 would be the same based on C_T concentrations normalized to
 604 a reference year—~~(not shown)~~. As noted by Touratier and Goyet (2009) the C_T concentrations in the

Mediterranean Sea should increase in parallel with the level of atmospheric anthropogenic CO₂. For an atmospheric CO₂ rate of +2.16 ppm yr⁻¹ over 1998-2023 (Lan et al., 2024) and at fixed sea surface temperature (17.75°C), salinity (38.25) and A_T (2567 μmol kg⁻¹), the theoretical C_T increase would be +1.24 μmol kg⁻¹ yr⁻¹. Interestingly, an anthropogenic flux of -0.3 ±0.02 molC m⁻² yr⁻¹ in the Mediterranean Sea (Bourgeois et al., 2016) would correspond to an increase of C_T of 1.07 ±0.07 μmol kg⁻¹ yr⁻¹ in the top 100 meters. This is again close to what is observed in winter or at 100m (Table 7, Figure 8). On the other hand the faster C_T trend observed in surface waters during summer might be associated with a decrease in biological production and/or changes in circulation/mixing over time that deserve specific investigations such as analyzed for the oxygen budget in this region (Ulses et al, 2021). It is worth noting that the C_T and A_T trends in coastal zones of the Mediterranean Sea are opposite to those observed offshore: for example at station SOLEMIO (Bay of Marseille, Wimart-Rousseau et al., 2020) the C_T and A_T concentrations decreased over 2016-2022 and thus opposed to the anthropogenic CO₂ signal, indicating that processes such as riverine inputs, advection or biology control the carbonate system decadal variability at local scale. This calls for developing dedicated complex biogeochemical models to resolve these processes (Barré et al., 2023, 2024), especially when extreme events occurred, such as the very hot summer in 2024 with SST up to 30°C in the Mediterranean Sea (Platforms Buoy/Mooring AZUR, EOL and La Revellata, data available at <https://dataselection.coriolis.eu.org/>). The data obtained in the Mediterranean Sea are important not only to validate biogeochemical models but also to reconstruct the carbonate system from A_T and pCO₂ data (Chau et al., 2024a) as the global A_T/SSS relationships (e.g. Carter et al., 2018) are not suitable for this region.

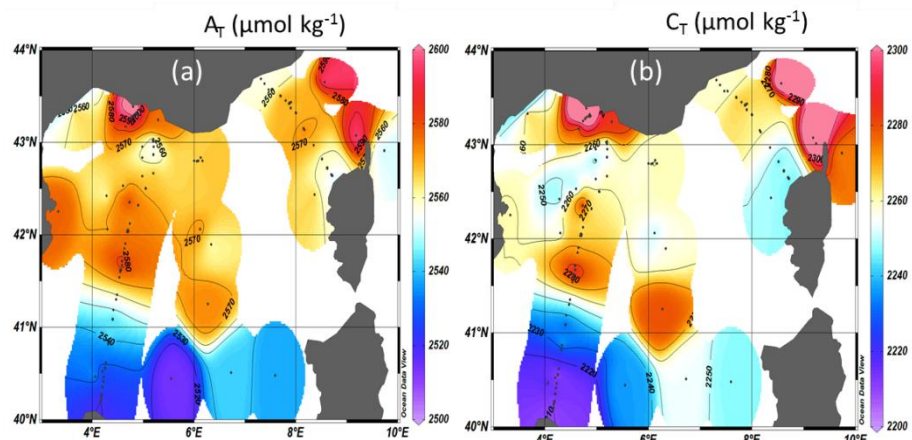
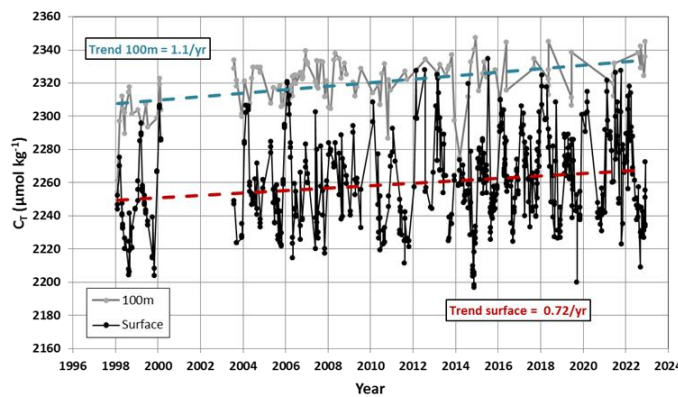


Figure 7: Distribution of A_T (a) and C_T (b) in μmol kg⁻¹ in surface waters of the Mediterranean Sea (0-10m) from observations over 2014-2023. Figures produced with ODV (Schlitzer, 2018).



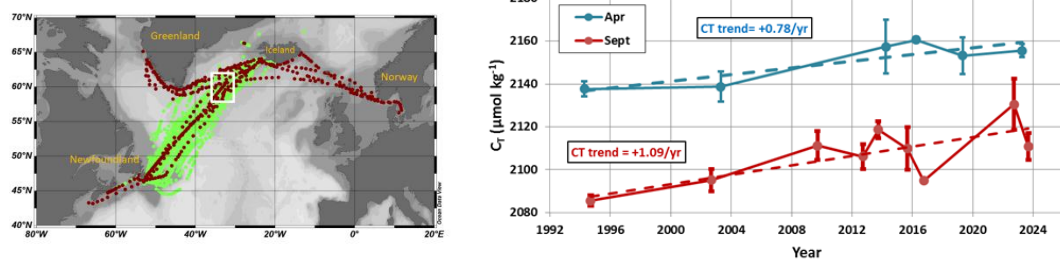
651
652
653 Figure 8: Time-series of C_T concentrations in surface (black symbols) and at 100m (grey symbols) in the
654 Ligurian Sea. The trends over 1998-2022 is surface (red) and at 100m (blue) are indicated by dashed lines.
655

656 **5.2 The North Atlantic**

658 The North Atlantic Ocean is an important CO₂ sink (Takahashi et al. 2009) due to biological activity
659 during summer, heat loss and deep convection during winter. As a result this region contains high concentrations
660 of anthropogenic CO₂ (C_{ant}) in the water column (Khatiwala et al., 2013). Decadal variations of the C_{ant}
661 inventories were recently identified at basin scale probably linked to the change of the overturning circulation
662 (Gruber et al., 2019; Müller et al., 2023; Pérez et al., 2024). This region experienced climate modes such as the
663 North Atlantic Oscillation (NAO) and the Atlantic Multidecadal Variability (AMV) that imprint variability in
664 air-sea CO₂ fluxes at inter-annual to multidecadal scales (e.g. Thomas et al., 2008; Jing et al., 2019;
665 Landschützer et al., 2019) but not always clearly revealed at regional scale (Metzl et al., 2010; Schuster et al.,
666 2013; Pérez et al., 2024). In addition it has been recently shown that extreme events such as the marine heat
667 wave in summer 2023 leaded to a reduce CO₂ uptake in this region (Chau et al., 2024b). Although the annual
668 CO₂ fluxes deduced from Global Ocean Biogeochemical Models (GOBM) seem coherent with the data-products
669 at basin scale (resp. -0.30 ± 0.07 and -0.24 ± 0.03 PgC/yr for the North Atlantic subpolar seasonally stratified,
670 NA-SPSS biome) the $p\text{CO}_2$ cycle seasonality is not well simulated (Pérez et al., 2024). Therefore to correct the
671 GOBMs outputs, comparisons with the observed C_T and A_T cycles are also needed.

672 In this context regular sampling in the North Atlantic (OVIDE cruises, Mercier et al., 2015, 2024;
673 SURATLANT transects, Reverdin et al., 2018) and time-series stations in the Irminger and Iceland Seas
674 (Ólafsson, et al., 2010; Lange et al., 2024; Yoder et al., 2024) are important to explore the variability of the
675 biogeochemical properties from seasonal (Figure S8) to decadal scales (Figure 9). The SURATLANT data added
676 in the SNAPO-CO₂-v2 dataset over 2017-2023 offer new observations in the North Atlantic Subpolar Gyre
677 (NASPG in the NA-SPSS biome) and new transects from Norway to Iceland and reaching the coast of Greenland
678 (Figure 9). In 2010 the winter NAO was negative, moved to a positive state in 2012-2020 and was again very
679 low in 2021. The new SURATLANT data after 2017 confirm the cooling and the freshening in the NASPG since
680 2009 (Holliday et al., 2020; Leseurre et al., 2020; Siddiqui et al., 2024) whereas the most recent data in 2022 and
681 2023 suggest a reverse trend (increase of salinity and temperature, ~~not shown~~Figure S8). After 2016, large C_T
682 anomalies in the NASPG were observed. For examples, in April 2019 and 2022, the C_T concentrations were low
683 compared to 2016 (Figure 9) and opposed to the expected anthropogenic CO₂ uptake. In September 2023 the C_T
684 concentrations were much lower than in 2022 (Figure 9) probably linked to biological productivity when the
685 NAO index was negative (Fröb et al., 2019) as observed in summer 2023 (NAO < -2 in July 2023). Despite these
686 variability the C_T trends are relatively well evaluated (Table 7). As in the Mediterranean Sea the C_T trends in the
687 NASPG appeared different depending on the season (Figure 9). The C_T increase was faster in September than in
688 April (resp. $+1.09 \pm 0.37 \mu\text{mol kg}^{-1} \text{ yr}^{-1}$ and $+0.78 \pm 0.23 \mu\text{mol kg}^{-1} \text{ yr}^{-1}$). This is either close to or lower than the
689 theoretical C_T increase due to the rising of atmospheric CO₂ ($+0.91 \mu\text{mol kg}^{-1} \text{ yr}^{-1}$) and in the range of recent
690 results evaluated for the Sub-polar Mode Waters in the Irminger Sea (C_{ant} trend = $0.95 \pm 0.17 \mu\text{mol kg}^{-1} \text{ yr}^{-1}$ for
691 the period 2009-2019, Curbelo-Hernández et al., 2024).

693
694
695
696
697
698
699
700
701
702



703 **Figure 9:** Left: Data in SNAPO-CO₂-v1 (green) and new data in v2 (brown) from the SURATLANT cruises in
704 1993–2023 in the North Atlantic. Figure produced with ODV (Schlitzer, 2018). The white box identified the
705 region of selected data around 60°N for the trend analysis. Right: Time-series of average C_T concentrations in
706 April (blue) and September (red) in this region. The trends for each season are indicated (see also Table 7).

708 5.3 The Tropical Atlantic

709

710 In the Tropical Atlantic, previous studies highlighted the large variability of biogeochemistry and the
711 difficulty in detecting long-term trends of C_T (e.g. Lefèvre et al., 2021). This is related to the variability of
712 circulation, equatorial upwelling, biological processes (some linked to Saharan dust) and inputs from large rivers
713 (Congo, Amazon and Orinoco). The new data added in version SNAPO-CO₂-v2 (Figure S9) show the
714 contrasting zonal C_T distribution in this region with lower concentrations in low salinity regions of the North
715 Equatorial Counter Current and Guinea Current (Figure 5; Oudot et al., 1995; Takahashi et al., 2014; Broullón et
716 al., 2020; Bonou et al., 2022). For exploring the temporal changes we selected the data in the western region
717 available for at least 10 years and separated the northern and southern sectors. In both regions the C_T trend is
718 close to $+3 \mu\text{mol kg}^{-1} \text{ yr}^{-1}$ (Table 7, Figure S9) much higher than the expected anthropogenic signal. In this
719 region where coastal water masses mixes with oceanic waters, the inter-annual variability of C_T is large and the
720 changes driven by competitive processes (circulation, biological processes). More observations and dedicated
721 models are needed to separate the anthropogenic and natural variability in this region (Pérez et al., 2024).

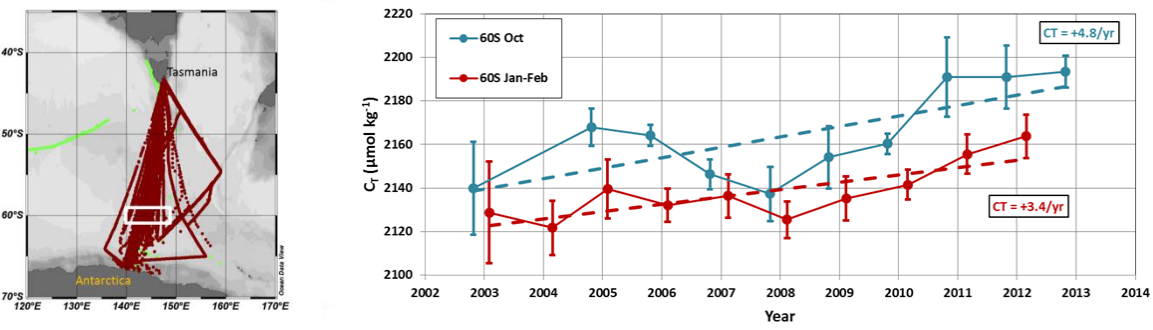
722

723 5.4 The Southern Ocean

724

725 In the Southern Ocean there are a few regular multi-annual observations of the carbonate system. Time
726 series of more than 10 years were obtained in the Drake Passage (Munro et al., 2015) and in the Southern Indian
727 Ocean (Leseurre et al., 2022; Metzl et al., 2024b). Observations were also obtained for more than 20 years
728 southeast of New Zealand at the Munida Time Series (MTS) in the subtropical and sub-Antarctic frontal zones
729 (Currie et al., 2011; Vance et al., 2024). To complement these datasets we have added the data collected in the
730 South-Eastern Indian Ocean between Tasmania and Antarctica in the frame of the MINERVE cruises (Figure 10;
731 Brandon et al., 2022). These cruises were conducted from October to March offering each year a view of the
732 seasonal changes between late winter and summer from the sub-Antarctic zone to the coastal zone near
733 Antarctica (Adélie land). In all sectors (here from 45°S to 67°S) the C_T concentrations were higher in October
734 when the mixed-layer depth (MLD) was deep and were lower during the productive summer season (e.g. Laika
735 et al., 2009; Shadwick et al., 2015). An example is presented at 60°S/151°E from the data obtained along a
736 reoccupied track in 2011–2012 (Figure S10). At this location south of the Polar Front in the POOZ/HNLC area

737 (Permanent Open Ocean Zone/ High Nutrient Low Chlorophyll), the C_T concentrations were $+25 \mu\text{mol kg}^{-1}$
 738 higher in October compared to February. The same seasonal amplitude was observed in the western Indian sector
 739 of the POOZ (Metzl et al., 2006, 2024b) suggesting that the C_T seasonality is relatively homogeneous in this
 740 region corresponding to the Indian SO-SPSS biome (Fay and McKinley, 2014). The difference in the
 741 climatological C_T between October and January is on average $+28.3 \pm 9.8 \mu\text{mol kg}^{-1}$ in the Indian Ocean POOZ
 742 (Takahashi et al., 2014). Given this seasonality and potential change in the seasonal amplitude over time
 743 (Gallego et al., 2018; Landschützer et al., 2018; Shadwick et al., 2023) the property trends have to be evaluated
 744 for October and January-February separately, here over 2002-2012 in the POOZ (Figure 10, Table 7). In both
 745 seasons, the average C_T concentrations reached a minimum in 2008 and increased faster in 2008-2012 (up to
 746 $+4.8 \mu\text{mol kg}^{-1} \text{ yr}^{-1}$). Interestingly, such acceleration of the trend after 2009 was observed for $p\text{CO}_2$ at the MTS
 747 station (Vance et al., 2024). We note that the C_T trend over 2002-2012 was slightly faster in October (Figure 10)
 748 probably linked to deeper MLD as suggested from the cooling and the salinity increase observed during this
 749 season ([not shown](#)[Figure S10](#)).



750
 751
 752
 753
 754
 755
 756
 757
 758
 759
 760
 761
Figure 10: Left: Data in SNAPO-CO₂-v1 dataset (green) and new data in version v2 (brown) in the South
 762 eastern Indian Ocean. Figure produced with ODV (Schlitzer, 2018). The white box identified the region of
 763 selected data around 60°S for the trend analysis. Right: Time-series of average C_T concentrations in January-
 764 February (red) and October (blue) around 60°S (white box in the map). The trends for each season are indicated
 765 (see also Table 7).

766 In the western Indian sector, the new data in the SNAPO-CO₂-v2 dataset from the OISO cruises at high
 767 latitudes also recorded a rapid C_T trend over 5-8 years periods (e.g., $+3.4 \mu\text{mol kg}^{-1} \text{ yr}^{-1}$ in 2015-2020 at 56°S,
 768 Figure 11, Table 7). Although the inter-annual variability of C_T , between 10 and 20 $\mu\text{mol kg}^{-1}$, is often
 769 recognized (Figure 11), the evaluation of the trends over more than 20 years indicated faster trend in the
 770 subtropical Indian Ocean ($+1.1 \mu\text{mol kg}^{-1} \text{ yr}^{-1}$) compared to higher latitudes (Indian POOZ, $+0.6 \mu\text{mol kg}^{-1} \text{ yr}^{-1}$);
 771 they are close to the expected anthropogenic signal in these regions ($+1.1 \mu\text{mol kg}^{-1} \text{ yr}^{-1}$ in the subtropics and
 772 $+0.8 \mu\text{mol kg}^{-1} \text{ yr}^{-1}$ at higher latitudes).

776
777
778
779
780
781
782
783
784
785
786
787
788
789
790

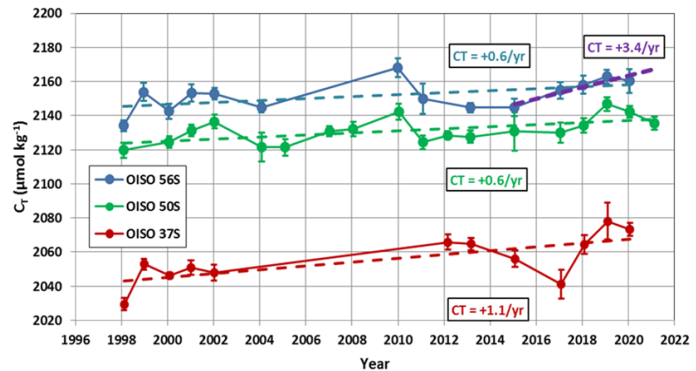
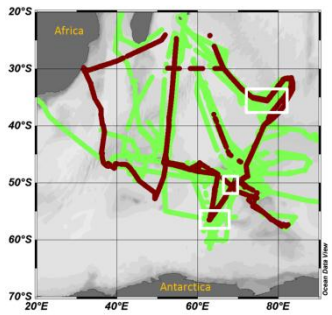


Figure 11: Left: Data in SNAPO-CO₂-v1 dataset (green) and new data in version v2 (brown) in the South Western Indian Ocean (OISO cruises). Figure produced with ODV (Schlitzer, 2018). The white boxes identified the regions of data selected around 37°S, 50°S and 56°S for the trend analysis. Right: Time-series of average C_T concentrations in January-February at 37°S (red), 50°S (green) and 56°S (blue). The trends for each region are indicated (see also Table 7).

Table 7: Trend of C_T ($\mu\text{mol kg}^{-1} \text{ yr}^{-1}$) and corresponding standard error in selected regions where data are available for more than 10 years. The projects/cruises for selection of the data in each domain are indicated.

Region	Period/Season	C_T trend ($\mu\text{mol kg}^{-1} \text{ yr}^{-1}$)	Projects/Cruises
North Atlantic (NASPG)	1994-2023 April	+0.78 (0.23)	SURATLANT
North Atlantic (NASPG)	1994-2023 September	+1.09 (0.37)	SURATLANT
West. Trop. Atl. 5N-Eq	2009-2021 April-October	+3.31 (2.13)	AMAZOMIX, PIRATA-BR, TARA
West. Trop. Atl. Eq-10S	2005-2015 April-October	+3.05 (1.64)	CAMFIN-WAT, PIRATA-BR, VOS
Ligurian Sea 8E	1998-2022 Jan-Feb.	+0.94 (0.64)	ANTARES, DYFAMED, MOOSE-GE
Ligurian Sea 8E	1998-2023 July-August	+1.53 (0.46)	ANTARES, DYFAMED, MOOSE-GE
Subtropical Indian 37S	1998-2020 Jan-Feb.	+1.12 (0.36)	OISO
South West. Indian 50S	1998-2021 Jan-Feb.	+0.61 (0.21)	OISO
South West. Indian 56S	1998-2020 Jan-Feb.	+0.58 (0.27)	OISO
South West. Indian 56S	2015-2020 Jan-Feb.	+3.41 (0.73)	OISO
South East. Indian 60S	2002-2012 Jan-Feb.	+3.37 (0.94)	MINERVE, OISO
South East. Indian 60S	2002-2012 October	+4.79 (1.62)	MINERVE

825 5.5 The Coastal Zones

826
827 Coastal waters experience enhanced ocean acidification due to increasing CO₂ uptake, accumulation of
828 anthropogenic CO₂ (Bourgeois et al 2016; Laruelle et al, 2018; Roobaert et al, 2024a; Li et al, 2024) and from
829 local anthropogenic inputs through rivers or from air pollution (e.g. Sarma et al, 2015; Sridvi and Sarma, 2021;
830 Wimart-Rousseau et al, 2020). The changes of the CO₂ uptake in coastal zones are also linked to biological
831 processes (Mathis et al, 2024) or to circulation and local upwelling (Roobaert et al, 2024b), all controlling large
832 variability of A_T and C_T in space and time leading to uncertainties for detecting long-term changes of $p\text{CO}_2$ and
833 air-sea CO₂ fluxes in heterogeneous coastal waters (Dai et al 2022; Resplandy et al, 2024). At seasonal scale,
834 large differences between observations and models were also identified leading to differences in the coastal

835 ocean CO₂ sink up to 60% (Resplandy et al, 2024). It is thus important to document the seasonal cycles of A_T and
836 C_T to compare and correct models and thus to better predict future changes of biogeochemical properties in
837 coastal waters and their impact on marine ecosystems. A better understanding of the processes and their
838 retroaction in the coastal regions is also required regarding Marine Carbone Dioxide Removal (MCDR)
839 experiments and for their evaluation (e.g. Ho et al, 2023).

840 In the SNAPO-CO₂-v2 dataset new data have been added in the coastal zones at stations SOMLIT-
841 Brest, SOMLIT-Roscoff and SOMLIT-Point-B. They extend the period to 2022 or 2023 for temporal analysis.
842 New data in the French coastal zones have been also included from the COCORICO₂ project documented in
843 detail by Petton et al (2024). The observations in coastal zones could be identified in the MARCATS regions
844 (Margins and CATchment Segmentation, Laruelle et al, 2013) (Figure 12) where little information is available
845 for quantifying the ocean CO₂ sink at the decadal scale and for evaluation of the anthropogenic CO₂ uptake
846 (Regnier et al, 2013; Dai et al, 2022; Li et al, 2024). To explore the change of the observed properties in the
847 coastal zones and have a flavor of the long-term C_T trends we selected the time series with at least 10 years of
848 data (Table 8, Figure 13). Except at high latitudes (Greenland and Antarctic coastal zones), we observed a
849 warming in coastal zones (~~not shown~~Figure S11). Changes in salinity are also identified (increase or decrease)
850 and results of the trends are presented for salinity-normalized C_T at 34, 35 or 38 depending on the region.
851 Although the inter-annual variability is large in coastal waters, sometimes linked to extreme events (e.g. river
852 discharges), we observed an increase in N-C_T at most of the 8 selected locations. The exceptions are the coastal
853 zones in the Gulf of Lion near the Rhone River and near Tasmania in October.

854 In the Gulf of Lion, the new data in the coastal zone confirmed the first view at the SOLEMIO station
855 over 2016-2018 (Bay of Marseille, Wimart-Rousseau et al, 2020). In this region the lowest C_T was observed in
856 summer 2022 (average C_T of $2238.6 \pm 21.0 \mu\text{mol kg}^{-1}$), much lower than in 2015 ($2290.8 \pm 44.7 \mu\text{mol kg}^{-1}$). Over
857 the continental shelf south of Tasmania (MARCATS #34), the trend in N-C_T was positive in summer but not
858 significant in October. In October this was associated with an increase in Salinity and in A_T probably linked to
859 advective processes via the reversal and variability of the Zeehan or the East Australian currents. From our data a
860 warming of $+0.06^\circ\text{C yr}^{-1}$ was identified for both seasons over 2002-2012 as previously observed south of
861 Tasmania over 1991-2003 impacting the pCO₂ trend and air-sea CO₂ fluxes in this region (Borges et al, 2008).
862 The difference in the N-C_T trends in austral summer and spring calls for new detailed studies with extended data
863 in this region. At high latitude in the Adélie Land (Antarctic coast MARCATS #45), the variability of N-C_T was
864 large (range from 2150 to 2200 $\mu\text{mol kg}^{-1}$, Figure 13) and the trend over 10 years in summer was not significant
865 (Table 8). As opposed to the open zone at 60°S (Figure 10) the C_T concentrations in the coastal zone near
866 Antarctica were not increasing, probably linked to competitive processes between anthropogenic uptake, changes
867 in primary production, mixing or ice melting (Shadwick et al, 2013, 2014). More data are needed to better
868 evaluate the changes of the carbonate system in Antarctic coastal zones where bottom waters are formed and
869 transport anthropogenic CO₂ at lower latitudes (Zhang et al, 2023).

870 For the coastal time series SOMLIT where annual trends could be estimated (sampling at monthly
871 resolution), the N-C_T increase ($+2.1$ to $3.4 \mu\text{mol kg}^{-1} \text{ yr}^{-1}$) is close or higher than the anthropogenic signal leading
872 to a decrease in pH ranging between -0.05 to -0.06 TS decade⁻¹. The new data added in the SNAPO-CO₂-v2
873 dataset (2016-2023) confirm the progressive increase in C_T and the acidification in the western Mediterranean
874 Sea and in the North-East Atlantic coastal zones (Kapsenberg et al, 2017; Gac et al, 2021).

875
876
877
878
879
880
881
882
883
884
885
886
887
888
889
890
891
892
893
894
895
896
897
898
899
900
901
902
903
904
905
906
907
908
909
910
911
912
913
914
915
916
917
918
919
920
921
922
923
924
925
926
927
928
929
930
931
932
933
934

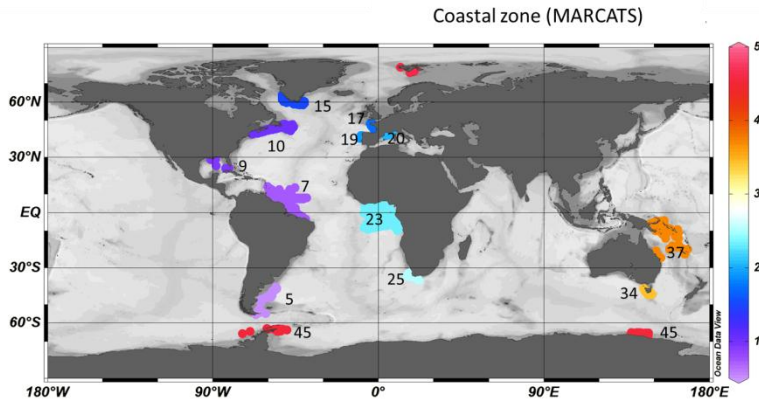


Figure 12: Location of A_T and C_T data available in the coastal zones in the SNAPO-CO₂-v2 dataset. Numbers and Color code identify MARCATS region (Laruelle et al, 2013). Figure produced with ODV (Schlitzer, 2018).

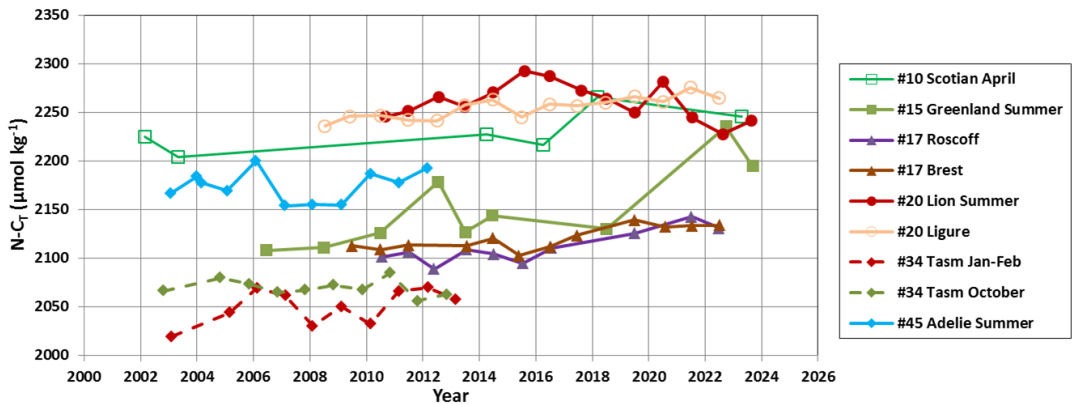


Figure 13: Time-series of average N- C_T concentrations ($\mu\text{mol kg}^{-1}$) in selected MARCATS regions for different period when data are available for ten years or more. The trends and periods for each region are indicated in Table 8.

Table 8: Trends of N- C_T ($\mu\text{mol kg}^{-1} \text{ yr}^{-1}$) and corresponding standard errors in selected coastal regions where data are available for 10 years or more. The projects/cruises for selection of the data in each domain are indicated. MARCATS # regions also identified. Salinity values used for C_T normalization are indicated.

Region #MARCATS	Period	Season	N- C_T Ttrend ($\mu\text{mol kg}^{-1} \text{ yr}^{-1}$)	Salinity	Projects/Cruises
Scotian #10	2002-2023	March-April	+1.71 (0.97)	35	SURATLANT
Greenland #15	2006-2023	June-mid-Sept	+5.77 (1.62)	35	OVIDE, SURATLANT
Roscoff #17	2010-2022	All season	+3.40 (0.76)	35	CHANNEL, COCORICO2, SOMLIT ROSCOFF
Bay of Brest #17	2009-2022	All seasons	+2.17 (0.52)	35	SOMLIT-Brest, COCORICO2, ECOSCPA,
LION#20	2010-2023	June-Sept	-1.19 (1.25)	38	COCORICO2, MOOSE-GE, SOLEMIO (a)
LIGURE#20	2008-2022	All seasons	+2.12 (0.36)	38	SOMLIT-Point-B, MOOSE-GE
Tasmania #34	2003-2013	Jan-Feb	+2.73 (1.72)	35	MINERVE, OISO
Tasmania #34	2002-2012	Oct	-0.65 (0.89)	35	MINERVE, OISO
Adélie #45	2002-2012	Dec-Feb	+0.63 (0.70)	34	MINERVE, OISO

(a) For LION, some data in summer were also used from punctual cruises: AMOR-BFlux, CARBORHONE, DICASE, LATEX, MESURHOBENT, MISSRHODIA2 and MOLA.

935 **6 Summary and suggestions**

936

937 This work extends in time and **in** new oceanic regions the A_T and C_T data presented in the first SNAPO-
 938 CO₂ synthesis (Metzl et al, 2024a). It includes now more than 67 000 surface and water column observations in
 939 all oceanic basins, in the Mediterranean Sea, in the coastal zones, near coral reefs, and in rivers. The data
 940 synthesized in version v2 are based on measurements of A_T and C_T performed between 1993 and 2023 with an
 941 accuracy of $\pm 4 \mu\text{mol kg}^{-1}$. Based on a secondary quality control, 91% of the A_T and C_T data are considered as
 942 good (WOCE Flag 2) and 6% probably good (Flag 3). For the open ocean this synthesis complements the
 943 SOCAT, GLODAP and SPOTS data products (Bakker et al., 2016; Lauvset et al., 2024; Lange et al, 2024). For
 944 the coastal sites this also complements the synthesis of coastal time-series in the Iberian Peninsula (Padin et al,
 945 2020), in the Canadian Atlantic continental shelf (Gibb et al, 2023) and around North America (Fassbender et al.,
 946 2018; Jiang et al., 2021; Jiang et al 2024, in prep). The SNAPO-CO₂ dataset enables to investigate the seasonal
 947 cycles, the inter-annual variability and the decadal trends of A_T and C_T in various oceanic provinces. The same
 948 temporal analyses could be investigated for other carbonate system properties such as $f\text{CO}_2$ or pH calculated
 949 from A_T and C_T for air-sea CO₂ flux estimates or ocean acidification studies (Figure 14).

950

951

952

953

954

955

956

957

958

959

960

961

962

963

964

965

966

967

968

969

970

971

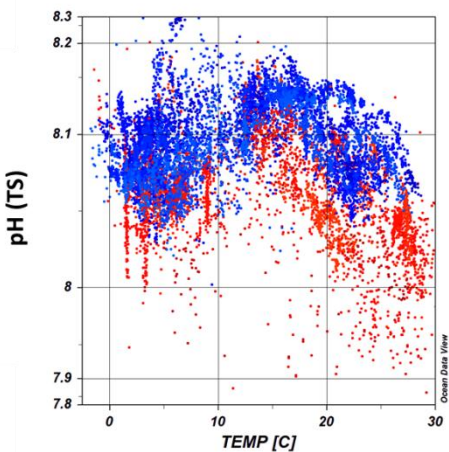


Figure 14: An example of observed ocean acidification derived from the SNAPO-CO₂-v2 dataset: pH (TS) calculated with A_T and C_T data are presented as a function of temperature (°C) for years 1998-2002 (blue symbols) and 2020-2023 (red symbols) and for salinity > 33 (Nb data selected with flag 2 = 11994). In recent years the pH was lower. Figure produced with ODV (Schlitzer, 2018).

972

973

974

975

976

977

978

979

980

981

In almost all regions the new data in 2021-2023 indicated that the C_T concentrations were higher in recent years. In regions where data are available for more than 2 decades, the time-series show an increase of sea surface C_T (North Atlantic, Southern Indian Ocean and Ligurian Sea) with a rate close to or higher than the changes expected from anthropogenic CO₂ uptake. It is also recognized that at seasonal scale the C_T trends could be different. However, with the data in hand, the long-term trend of C_T cannot be quantified with confidence to compare with the anthropogenic carbon uptake in some regions. This is the case in the eastern tropical Atlantic subject to high inter-annual variability (Lefèvre et al., 2021, 2024) although new data have been added over 2005-2022 in this region (Table 1, Figure S9). When data are available for less than a decade the increase in C_T was observed but the trend was uncertain due to large inter-annual variability (e.g. Adélie Land). An exception was identified in the coastal zone in the Gulf of Lion (Mediterranean Sea) where summer data since 2010 present

982 a decrease in C_T most pronounced since 2015 (C_T trend = $-5.2 \pm 1.5 \text{ } \mu\text{mol kg}^{-1} \text{ yr}^{-1}$). Such C_T decrease over 10
983 years was also observed at the Hawaii Ocean Time series, HOT over 2010-2020 (Dore et al, 2009,
984 <https://hahana.soest.hawaii.edu/hot/hotco2/hotco2.html>, last access: 27 August 2024).

985 Although the A_T concentrations present significant inter-annual variability such as in the NASPG, in the
986 Topical Atlantic or the Adélie land and coastal zones, A_T appears relatively constant over time except at these
987 locations. In the open ocean, we observed an increase of A_T in the Southern Ocean south of the Polar Front
988 around 60°S in 2003-2012 not directly linked to salinity. In the coastal zones a decrease of A_T was pronounced
989 south of Greenland. In the coast in the Gulf of Lion, as observed for C_T , A_T decreased (A_T trend = $-2.8 \pm 1.2 \text{ } \mu\text{mol}$
990 $\text{kg}^{-1} \text{ yr}^{-1}$). This is opposed to the changes observed in the Ligurian Sea at station SOMLIT-Point-B, where C_T and
991 A_T increased over 2007-2015 (Kapsenberg et al, 2017) highlighting the contrasting C_T and A_T trends in the
992 Mediterranean coastal zones where ocean acidification is detected (here over 2008-2022, pH trend of -0.048
993 $\pm 0.003 \cdot \text{decade}^{-1}$). With the continuous warming, reduced stratification and the rapid pH change observed in the
994 Mediterranean Sea, how the marine ecosystems will respond in the future should be addressed (e.g. Howes et al,
995 2015; Maugendre et al 2015; Lacoue-Labarthe et al, 2016). The SNAPO-CO2-v2 dataset could also be used to
996 explore and analyze the changes of the carbonate system occurring during extreme events such as marine heat
997 waves, rapid freshening, deep convection or high phytoplankton bloom events.

998 This dataset could also serve for validating autonomous platforms capable of measuring pH and $f\text{CO}_2$
999 properties (Sarmiento et al, 2023) and, along with other synthesis products (Jiang et al, 2024 in prep.), provides
1000 an additional reference dataset for the development and validation of regional biogeochemical models for
1001 simulating air-sea CO_2 fluxes. Thanks to the RECCAP2 stories, it has been recognized that Ocean
1002 Biogeochemical Models present biases in the seasonal cycle of C_T and A_T due to inadequate representation of
1003 biogeochemical cycles (e.g. Hauck et al, 2023; Rodgers et al, 2023; Sarma et al, 2023; Pérez et al, 2024;
1004 Resplandy et al, 2024). The SNAPO-CO2-v2 dataset could be used to guide analyses for regional or global
1005 biogeochemical models for A_T and C_T comparison and validation from seasonal to decadal scales. Our dataset is
1006 also essential for training and validating neural networks capable of predicting variables in the carbonate system
1007 (e.g. Fourier et al, 2020; Chau et al, 2024a; Gregor et al, 2024), thereby enhancing observations of marine CO_2 at
1008 different spatial and temporal scales. Furthermore, we encourage the use of this dataset (or part of it), at sea or
1009 prior going to sea for cruise planning. Indeed, using the approach of Davis and Goyet (2021) which takes into
1010 account the multiple constraints (ship-time, number of samples, etc.), it is possible to determine the most
1011 appropriate sampling strategy (Guglielmi et al., 2022, 2023), to reach the specific scientific objectives of each
1012 cruise.

1013 The data presented here are available online on the Seanoe servor (<https://doi.org/10.17882/102337>) in a
1014 file identifying version v1 and v2. The sources of the original datasets (doi) with the associated references are
1015 listed in the Supplementary Material (Tables S3, S4). As for version v1 we invite the users to comment on any
1016 anomaly that would have not been detected or to suggest potential misqualification of data in the present product
1017 (e.g. data probably good although assigned with flag 3, probably wrong). As for SOCAT or GLODAP, we
1018 expect to update the SNAPO-CO2 dataset once new observations are obtained and controlled.

1019
1020 **7 Data availability**

1021 Data presented in this study are available at Seanoe (Metzl et al, 2024d, <https://www.seanoe.org>,
1022 <https://doi.org/10.17882/102337>. See also <https://doi.org/10.17882/95414> for version V1. The dataset is also
1023 available at <https://explore.webodv.awi.de/ocean/carbon/snapo-co2/>

1024

1025 *Author contributions.* NM prepared the data synthesis, the figures and wrote the draft of the manuscript with
1026 contributions from all authors. JF measured the discrete samples since 2014, with the help from CM and CLM,
1027 and prepared the individual reports for each project. NM and JF pre-qualified the discrete A_T/C_T data. CLM and
1028 NM are co-Is of the ongoing OISO project and qualified the underway A_T/C_T data from OISO cruises. FT and
1029 CG were PIs of the MINERVE cruises. All authors have contributed either to organizing cruises, sample
1030 collection and/or data qualification, and reviewed the manuscript.

1031

1032 *Competing interest.* The authors have the following competing interests: At least one of the (co-)authors is a
1033 member of the editorial board of Earth System Science Data

1034

1035 *Acknowledgments.* Most of the A_T and C_T data presented in this study were measured at the SNAPO-CO2 facility
1036 (Service National d'Analyse des Paramètres Océniques du CO2) housed by the LOCEAN laboratory and part of
1037 the OSU ECCE Terra at Sorbonne University and INSU/CNRS analytical services. Support by INSU/CNRS, by
1038 OSU ECCE Terra and by LOCEAN, is gratefully acknowledged as well as support by different French “Services
1039 nationaux d’Observations”, such as OISO/CARAUS, SOMLIT, PIRATA, SSS and MOOSE. We thank the
1040 research infrastructure ICOS (Integrated Carbon Observation System) France for funding a large part of the
1041 analyses. We thank the IRD (Institut de Recherche pour le Développement) and the French-Brazilian IRD-
1042 FAPEMA program for funding observations in the tropical Atlantic. We thank the French oceanographic fleet
1043 (“Flotte océanographique française”) for financial and logistic support for most cruises listed in this synthesis
1044 and for the OISO program (<https://campagnes.flotteoceanographique.fr/series/228/>). We acknowledge the
1045 MOOSE program (Mediterranean Ocean Observing System for the Environment,
1046 <https://campagnes.flotteoceanographique.fr/series/235/fr/>) coordinated by CNRS-INSU and the Research
1047 Infrastructure ILICO (CNRS-IFREMER). The CocoriCO2 project was founded by European Maritime and
1048 Fisheries Fund (grant no. 344, 2020–2023) and benefited from a subsidy from the Adour-Garonne water agency.
1049 We thank the following programs coordinated by A. Tribollet which have contributed to the acquisition of the
1050 data in Mayotte: CARBODISS funded by CNRS-INSU in 2018-2019, Future Maore reefs funded by Next
1051 Generation UE-France Relance in 2021-2023, and OA-ME funded by a Belmont Forum International (ANR) in
1052 2020-2026. We thank the program Mermex-Mistral CNRS for supporting AMOR-BFlux, CARBORHONE,
1053 DICASE and MESURHOBENT cruises and the program EC2CO-INSU for supporting MISSRHODIA2 cruise.
1054 The ACCESS project was supported by CNRS MISTRALS and the DELTARHONE-1 by EC2CO-INSU. The
1055 ACIDHYPO project was founded by CNRS International Emerging Actions; we thank Captain and crew of the
1056 R/V Savannah from the Skidaway Institute of Oceanography (University of Georgia) for their support and
1057 technical assistance during the operations at sea. The AMAZOMIX project was funded by French
1058 Oceanographic Fleet, INSU (LEFE), IRD (LMI TAPICOA), CNES (TOSCA MIAMAZ project) and by the
1059 French-Brazilian international program GUYAMAZON. The OISO program was supported by the French
1060 institutes INSU (Institut National des Sciences de l’Univers) and IPEV (Institut Polaire Paul-Emile Victor), OSU

1061 Ecce-Terra (at Sorbonne Université), and the French program SOERE/Great-Gases. We also thank the Research
1062 Infrastructure ILICO (<https://www.ir-ilico.fr>). We warmly thank Alain Poisson who initiated the MINERVE
1063 program and performed many of the measurements onboard R/V Astrolabe from 2002 through 2018. We thank
1064 all colleagues and students who participated to the cruises and have carefully collected the precious seawater
1065 samples. We thank Frédéric Merceur (IFREMER) for preparing the page and data availability on Seanoe and
1066 Reiner Schlitzer (AWI) for including the SNAPO-CO₂ dataset in the ODV portal. We thank the associated editor
1067 Sebastiaan van de Velde to manage this manuscript, and Kim Currie and Toste Tanhua for their suggestions that
1068 helped to improve this article.

1069

1070 **References:**

1071

1072 Ait Ballagh, F.E., Rabouille, C., Andrieux-Loyer, F. et al. Spatial Variability of Organic Matter and Phosphorus
1073 Cycling in Rhône River Prodelta Sediments (NW Mediterranean Sea, France): a Model-Data Approach.
1074 Estuaries and Coasts 44, 1765–1789, <https://doi.org/10.1007/s12237-020-00889-9>, 2021

1075

1076 Álvarez, M., Catalá, T. S., Civitarese, G., Coppola, L., Hassoun, A. E.R., Ibello, V., Lazzari, P., Lefevre, D.,
1077 Macías, D., Santinelli, C. and Ulses, C.: Chapter 11 - Mediterranean Sea general biogeochemistry, Editor(s):
1078 Katrin Schroeder, Jacopo Chiggiato, Oceanography of the Mediterranean Sea, Elsevier, Pages 387-451,
1079 <https://doi.org/10.1016/B978-0-12-823692-5.00004-2>, 2023.

1080

1081 Bakker, D. C. E., Pfeil, B., Landa, C. S., Metzl, N., O'Brien, K. M., Olsen, A., Smith, K., Cosca, C., Harasawa,
1082 S., Jones, S. D., Nakaoka, S.-I., Nojiri, Y., Schuster, U., Steinhoff, T., Sweeney, C., Takahashi, T., Tilbrook, B.,
1083 Wada, C., Wanninkhof, R., Alin, S. R., Balestrini, C. F., Barbero, L., Bates, N. R., Bianchi, A. A., Bonou, F.,
1084 Boutin, J., Bozec, Y., Burger, E. F., Cai, W.-J., Castle, R. D., Chen, L., Chierici, M., Currie, K., Evans, W.,
1085 Featherstone, C., Feely, R. A., Fransson, A., Goyet, C., Greenwood, N., Gregor, L., Hankin, S., Hardman-
1086 Mountford, N. J., Harley, J., Hauck, J., Hoppema, M., Humphreys, M. P., Hunt, C. W., Huss, B., Ibánhez, J. S.
1087 P., Johannessen, T., Keeling, R., Kitidis, V., Körtzinger, A., Kozyr, A., Krasakopoulou, E., Kuwata, A.,
1088 Landschützer, P., Lauvset, S. K., Lefèvre, N., Lo Monaco, C., Manke, A., Mathis, J. T., Merlinat, L., Millero, F.
1089 J., Monteiro, P. M. S., Munro, D. R., Murata, A., Newberger, T., Omar, A. M., Ono, T., Paterson, K., Pearce, D.,
1090 Pierrot, D., Robbins, L. L., Saito, S., Salisbury, J., Schlitzer, R., Schneider, B., Schweitzer, R., Sieger, R.,
1091 Skjelvan, I., Sullivan, K. F., Sutherland, S. C., Sutton, A. J., Tadokoro, K., Telszewski, M., Tuma, M., Van
1092 Heuven, S. M. A. C., Vandemark, D., Ward, B., Watson, A. J., and Xu, S.: A multi-decade record of high-quality
1093 fCO₂ data in version 3 of the Surface Ocean CO₂ Atlas (SOCAT), Earth Syst. Sci. Data, 8, 383-413,
1094 doi:10.5194/essd-8-383-2016. 2016.

1095

1096 Barral, Q-B., Zakardjian, B., Dumas, F., Garreau, P., Testor, P., and Beuvier, J.: Characterization of fronts in the
1097 Western Mediterranean with a special focus on the North Balearic Front, Progress in Oceanography, Volume
1098 197, 102636, <https://doi.org/10.1016/j.pocean.2021.102636>. 2021

1099

1100 Barré, L., Diaz, F., Wagener, T., Van Wambeke, F., Mazoyer, C., Yohia, C., and Pinazo, C.: Implementation and
1101 assessment of a model including mixotrophs and the carbonate cycle (Eco3M_MIX-CarbOx v1.0) in a highly
1102 dynamic Mediterranean coastal environment (Bay of Marseille, France) – Part 1: Evolution of ecosystem
1103 composition under limited light and nutrient conditions, Geosci. Model Dev., 16, 6701–6739,
1104 <https://doi.org/10.5194/gmd-16-6701-2023>, 2023.

1105

1106 Barré, L., Diaz, F., Wagener, T., Mazoyer, C., Yohia, C., and Pinazo, C.: Implementation and assessment of a
1107 model including mixotrophs and the carbonate cycle (Eco3M_MIX-CarbOx v1.0) in a highly dynamic
1108 Mediterranean coastal environment (Bay of Marseille, France) – Part 2: Towards a better representation of total
1109 alkalinity when modeling the carbonate system and air-sea CO₂ fluxes, Geosci. Model Dev., 17, 5851–5882,
1110 <https://doi.org/10.5194/gmd-17-5851-2024>, 2024.

1111

1112 BERTRAND Arnaud, DE SAINT LEGER Emmanuel, KOCH-LARROUY Ariane : AMAZOMIX 2021 cruise,
1113 RV Antea, <https://doi.org/10.17600/18001364>, 2021

- 1114
1115 Bitting, H.C., Steinhoff, T., Claustre, H., Fiedler, B., Williams, N.L., Sauzède, R., Körtzinger, A. and Gattuso, J.-
1116 P.: An Alternative to Static Climatologies: Robust Estimation of Open Ocean CO₂ Variables and Nutrient
1117 Concentrations From T, S, and O₂ Data Using Bayesian Neural Networks. *Front. Mar. Sci.* 5:328. doi:
1118 10.3389/fmars.2018.00328, 2018
1119
1120 Bonou, F.K., Noriega, C., Lefèvre, N., Araujo, M.: Distribution of CO₂ parameters in the Western Tropical
1121 Atlantic Ocean, *Dynamics of Atmospheres and Oceans*, 73: 47-60
1122 <http://dx.doi.org/10.1016/j.dynatmoce.2015.12.001>, 2016
1123
1124 Bonou, F., Medeiros, C., Noriega, C., Araujo, M., Aubains Hounso-Gbo, A., and Lefèvre N. : A comparative
1125 study of total alkalinity and total inorganic carbon near tropical Atlantic coastal regions. *J Coast Conserv* 26, 31,
1126 <https://doi.org/10.1007/s11852-022-00872-5>, 2022
1127
1128 Borges A.V., B. Tilbrook, N. Metzl, A. Lenton and B. Delille: Inter-annual variability of the carbon dioxide
1129 oceanic sink south of Tasmania, *Biogeosciences*, 5, 141-155. <https://doi.org/10.5194/bg-5-141-2008>, 2008
1130
1131 Bourgeois, T., J. C. Orr, L. Resplandy, J. Terhaar, C. Ethé, M. Gehlen, and L. Bopp: Coastal-ocean uptake of
1132 anthropogenic carbon. *Biogeosciences*, 13, 4167-4185, doi: 10.5194/bg-13-4167-2016., 2016
1133
1134 BOURLES Bernard (1997) PIRATA, <https://doi.org/10.18142/14>
1135
1136 BOURLES Bernard (2019) PIRATA FR29 cruise, RV Thalassa, <https://doi.org/10.17600/18000875>
1137
1138 BOURLES Bernard, LLIDO Jérôme (2020) PIRATA FR30 cruise, RV Thalassa,
1139 <https://doi.org/10.17600/18000690>
1140
1141 BOURLES Bernard, LLIDO Jérôme (2022) PIRATA FR32 cruise, RV Thalassa,
1142 <https://doi.org/10.17600/18001832>
1143
1144 Bozec Y., Cariou, T., Mace, E., Morin, P., Thuillier, D., Vernet, M.: Seasonal dynamics of air-sea CO₂ fluxes in
1145 the inner and outer Loire estuary (NW Europe). *Estuarine Coastal And Shelf Science*, 100, 58-71.
1146 <https://doi.org/10.1016/j.ecss.2011.05.015>, 2012
1147
1148 BOZEC Yann (2009) CO2ARVOR 3 cruise, RV Côtes De La Manche, <https://doi.org/10.17600/9480170>
1149
1150 BOZEC Yann (2009) CO2ARVOR 2 cruise, RV Côtes De La Manche, <https://doi.org/10.17600/9480110>
1151
1152 BOZEC Yann (2009) CO2ARVOR 1 cruise, RV Thalia, <https://doi.org/10.17600/9070070>
1153
1154 Brandon, M., C. Goyet, F. Touratier, N. Lefèvre, E. Kestenare, and R. Morrow : Spatial and temporal variability
1155 of the physical, carbonate and CO₂ properties in the Southern Ocean surface waters during austral summer
1156 (2005-2019). *Deep Sea Res. Part I*, 187, 103836, <https://doi.org/10.1016/j.dsri.2022.103836>. 2022
1157
1158 Broullón, D., Pérez, F. F., Velo, A., Hoppema, M., Olsen, A., Takahashi, T., Key, R. M., Tanhua, T., González-
1159 Dávila, M., Jeansson, E., Kozyr, A., and van Heuven, S. M. A. C.: A global monthly climatology of total
1160 alkalinity: a neural network approach, *Earth Syst. Sci. Data*, 11, 1109–1127, <https://doi.org/10.5194/essd-11-1109-2019>. 2019
1161
1162 Broullón, D., Pérez, F. F., Velo, A., Hoppema, M., Olsen, A., Takahashi, T., Key, R. M., Tanhua, T., Santana-
1163 Casiano, J. M., and Kozyr, A.: A global monthly climatology of oceanic total dissolved inorganic carbon: a
1164

- 1165 neural network approach, *Earth Syst. Sci. Data*, 12, 1725–1743, <https://doi.org/10.5194/essd-12-1725-2020>.
1166 2020
1167
1168 CARIOU Thierry, BOZEC Yann (2010) CO2ARVOR 4 cruise, RV Thalia, <https://doi.org/10.17600/10070040>
1169
1170 Carter, B. R., Feely, R. A., Williams, N. L., Dickson, A. G., Fong, M. B., and Takeshita, Y.: Updated methods
1171 for global locally interpolated estimation of alkalinity, pH, and nitrate. *Limnology and Oceanography: Methods*,
1172 16: 119–131. doi: 10.1002/lom3.10232, 2018
1173
1174 Chau, T.-T.-T., Gehlen, M., Metzl, N., and Chevallier, F.: CMEMS-LSCE: a global, 0.25°, monthly
1175 reconstruction of the surface ocean carbonate system, *Earth Syst. Sci. Data*, 16, 121–160,
1176 <https://doi.org/10.5194/essd-16-121-2024>, 2024a.
1177
1178 Chau, T.-T.-T., Chevallier, F., and Gehlen, M.: Global analysis of surface ocean CO₂ fugacity and air-sea fluxes
1179 with low latency. *Geophysical Research Letters*, 51, e2023GL106670. <https://doi.org/10.1029/2023GL106670>,
1180 2024b
1181
1182 Cheng, L. J., Abraham, J., Zhu, J., Trenberth, K. E., Fasullo, J., Boyer, T., Locarnini, R., Zhang, B., Yu, F. J.,
1183 Wan, L. Y., Chen, X. R., Song, X. Z., Liu, Y. L., and Mann, M. E.: Record-setting ocean warmth continued in
1184 2019, *Adv. Atmos. Sci.*, 37, 137–142. <https://doi.org/10.1007/s00376-020-9283-7>, 2020
1185
1186 Cheng, L., Abraham, J., Trenberth, K.E. et al. New Record Ocean Temperatures and Related Climate Indicators
1187 in 2023. *Adv. Atmos. Sci.*, <https://doi.org/10.1007/s00376-024-3378-5>, 2024
1188
1189 Conan, P., Guieux, A., and Vuillemin, R.: MOOSE (MOLA), <https://doi.org/10.18142/234>, 2020.
1190
1191 Copin-Montégut, C.: Alkalinity and carbon budgets in the Mediterranean Sea, *Global Biogeochemical Cycles*,
1192 vol. 7, pp. 915–925, 1993.
1193
1194 Coppola, L., and Diamond-Riquier, E.: MOOSE (DYFAMED), <https://doi.org/10.18142/131>, 2008.
1195
1196 Coppola Laurent, Diamond Riquier Emilie, Carval Thierry, Irisson Jean-Olivier, Desnos Corinne: Dyfamed
1197 observatory data. SEANOE. <https://doi.org/10.17882/43749>, 2024
1198
1199 Coppola, L., Fourrier, M., Pasqueron de Fommervault, O., Poteau, A., Riquier, E. D. and Béguery, L.:
1200 Highresolution study of the air-sea CO₂ flux and net community oxygen production in the Ligurian Sea by a
1201 fleet of gliders. *Front. Mar. Sci.* 10:1233845. doi: 10.3389/fmars.2023.1233845, 2023
1202
1203 Curbelo-Hernández, D., Pérez, F. F., González-Dávila, M., Gladyshev, S. V., González, A. G., González-
1204 Santana, D., Velo, A., Sokov, A., and Santana-Casiano, J. M.: Ocean Acidification trends and Carbonate System
1205 dynamics in the North Atlantic Subpolar Gyre during 2009–2019, *EGUsphere* [preprint],
1206 <https://doi.org/10.5194/egusphere-2024-1388>, 2024.
1207
1208 Currie, K. I., Reid, M. R., and Hunter, K. A.: Interannual variability of carbon dioxide draw-down by
1209 subantarctic surface water near New Zealand, *Biogeochemistry*, 104, 23–34, <https://doi.org/10.1007/s10533-009-9355-3>, 2011.
1211
1212 Cyronak, T., Santos, I. R., Erler, D. V., and Eyre, B. D.: Groundwater and porewater as major sources of
1213 alkalinity to a fringing coral reef lagoon (Muri Lagoon, Cook Islands), *Biogeosciences*, 10, 2467–2480,
1214 <https://doi.org/10.5194/bg-10-2467-2013>, 2013.
1215
1216 Dai, M., J. Su, Y. Zhao, E. E. Hofmann, Z. Cao, W. -J. Cai, J. Gan, F. Lacroix, G. G. Laruelle, F. Meng, J. D.
1217 Müller, P. A.G. Regnier, G. Wang, Z. Wang, 2022. Carbon Fluxes in the Coastal Ocean: Synthesis, Boundary

- 1218 Processes and Future Trends, Annual Review of Earth and Planetary Sciences, 50:1, 593-626,
1219 <https://doi.org/10.1146/annurev-earth-032320-090746>, 2022
- 1220
- 1221 Davis D. and Goyet, C.: Balanced Error Sampling with applications to ocean biogeochemical sampling.
1222 Collection études, Presses Universitaires de Perpignan, 224p. ISBN : 978-2-35412-452-6, 2021
- 1223
- 1224 Dickson, A. G., Sabine, C. L., and Christian, J. R.: Guide to best practices for ocean CO₂ measurements, North
1225 Pacific Marine Science Organization, Sidney, British Columbia, 191, <https://doi.org/10.25607/OBP-1342>, 2007.
- 1226
- 1227 DOE: Handbook of Methods for Analysis of the Various Parameters of the Carbon Dioxide System in Seawater;
1228 version 2, A.G. Dickson et C. Goyet, eds, ORNL/CDIAC-74, <https://doi.org/10.2172/10107773>, 1994.
- 1229
- 1230 Doney, S. C., Fabry, V. J., Feely, R. A., and Kleypas, J. A., Ocean acidification: The other CO₂ problem. *Annual
1231 Review of Marine Science*, 1(1), 169–192. 10.1146/annurev.marine.010908.163834, 2009
- 1232
- 1233 Doney, S. C., Busch, D. S., Cooley, S. R., and Kroeker, K. J.: The Impacts of Ocean Acidification on Marine
1234 Ecosystems and Reliant Human Communities. *Annual Review of Environment and Resources* 45:1,
1235 <https://doi.org/10.1146/annurev-environ-012320-083019>. 2020
- 1236
- 1237 Dumoulin J-P, Pozzato L., Rassman J., Toussaint F., Fontugne M., Tisnerat-Laborde N., Beck L., Caffy I.,
1238 Delqué-Kolic E., Moreau C., Rabouille C. : Isotopic Signature (13C, 14C) of DIC in Sediment Pore Waters: An
1239 Example from the Rhone River Delta. Radiocarbon, 60(5), 1465-1481. <https://doi.org/10.1017/RDC.2018.111>,
1240 2018.
- 1241
- 1242 Dumoulin J-P, Rabouille C, Pourtout S, Bomblet B, Lansard B, Caffy I, Hain S, Perron M, Sieudat M, Thellier
1243 B, Delqué-Koli E, Moreau C, Beck L (2022). : Identification in Pore Waters of Recycled Sediment Organic
1244 Matter Using the Dual Isotopic Composition of Carbon (13C and 14C): New Data From the Continental Shelf
1245 Influenced by the Rhône River. Radiocarbon, 64(6), 1617-1627. <https://doi.org/10.1017/RDC.2022.71>, 2022.
- 1246
- 1247 Edmond, J. M.: High precision determination of titration alkalinity and total carbon dioxide content of sea water
1248 by potentiometric titration, Deep-Sea Res., 17, 737–750, [https://doi.org/10.1016/0011-7471\(70\)90038-0](https://doi.org/10.1016/0011-7471(70)90038-0), 1970.
- 1249
- 1250 Eyring, V., Righi, M., Lauer, A., Evaldsson, M., Wenzel, S., Jones, C., Anav, A., Andrews, O., Cionni, I., Davin,
1251 E. L., Deser, C., Ehbrecht, C., Friedlingstein, P., Gleckler, P., Gottschaldt, K.-D., Hagemann, S., Juckes, M.,
1252 Kindermann, S., Krasting, J., Kunert, D., Levine, R., Loew, A., Mäkelä, J., Martin, G., Mason, E., Phillips, A. S.,
1253 Read, S., Rio, C., Roehrig, R., Senftleben, D., Sterl, A., van Ulft, L. H., Walton, J., Wang, S., and Williams, K.
1254 D.: ESMValTool (v1.0) – a community diagnostic and performance metrics tool for routine evaluation of Earth
1255 system models in CMIP, Geosci. Model Dev., 9, 1747-1802, doi:10.5194/gmd-9-1747-2016, 2016.
- 1256
- 1257 Fabry, V. J., Seibel, B. A., Feely, R. A. and Orr, J. C.: Impacts of ocean acidification on marine fauna and
1258 ecosystem processes. *ICES J. Mar. Sci.* 65, 414–432. <https://doi.org/10.1093/icesjms/fsn048>, 2008.
- 1259
- 1260 Faranda, D., Pascale, S., Bulut, B.: Persistent anticyclonic conditions and climate change exacerbated the
1261 exceptional 2022 European-Mediterranean drought. *Environ. Res. Lett.*, 18, 034030, DOI 10.1088/1748-
1262 9326/acbc37, 2023
- 1263
- 1264 Fassbender, A. J., Alin, S. R., Feely, R. A., Sutton, A. J., Newton, J. A., Krembs, C., Bos, J., Keyzers, M., Devol,
1265 A., Ruef, W., and Pelletier, G.: Seasonal carbonate chemistry variability in marine surface waters of the US
1266 Pacific Northwest, *Earth Syst. Sci. Data*, 10, 1367–1401, <https://doi.org/10.5194/essd-10-1367-2018>, 2018.
- 1267
- 1268 Fay, A. R., and McKinley, G. A.: Global open-ocean biomes: Mean and temporal variability. *Earth System
1269 Science Data*, 6(2), 273–284. <https://doi.org/10.5194/essd-6-273-2014>, 2014

- 1270
1271 Fourrier, M., Coppola, L., Claustre, H., D'Ortenzio, F., Sauzède, R. and Gattuso, J.-P.: A regional neural
1272 network approach to estimate water-column nutrient concentrations and carbonate system variables in the
1273 Mediterranean Sea: CANYON-MED. *Frontiers in Marine Science*, 7:620,
1274 <https://www.frontiersin.org/articles/10.3389/fmars.2020.00620>, 2020.
1275
1276 Friedlingstein, P., O'Sullivan, M., Jones, M. W., Andrew, R. M., Gregor, L., Hauck, J., Le Quéré, C., Luijkx, I.
1277 T., Olsen, A., Peters, G. P., Peters, W., Pongratz, J., Schwingshackl, C., Sitch, S., Canadell, J. G., Ciais, P.,
1278 Jackson, R. B., Alin, S. R., Alkama, R., Arneth, A., Arora, V. K., Bates, N. R., Becker, M., Bellouin, N., Bittig,
1279 H. C., Bopp, L., Chevallier, F., Chini, L. P., Cronin, M., Evans, W., Falk, S., Feely, R. A., Gasser, T., Gehlen,
1280 M., Gkritzalis, T., Gloege, L., Grassi, G., Gruber, N., Gürses, Ö., Harris, I., Hefner, M., Houghton, R. A., Hurtt,
1281 G. C., Iida, Y., Ilyina, T., Jain, A. K., Jersild, A., Kadono, K., Kato, E., Kennedy, D., Klein Goldewijk, K.,
1282 Knauer, J., Korsbakken, J. I., Landschützer, P., Lefèvre, N., Lindsay, K., Liu, J., Liu, Z., Marland, G., Mayot, N.,
1283 McGrath, M. J., Metzl, N., Monacci, N. M., Munro, D. R., Nakaoka, S.-I., Niwa, Y., O'Brien, K., Ono, T.,
1284 Palmer, P. I., Pan, N., Pierrot, D., Pocock, K., Poulter, B., Resplandy, L., Robertson, E., Rödenbeck, C.,
1285 Rodriguez, C., Rosan, T. M., Schwinger, J., Séférian, R., Shutler, J. D., Skjelvan, I., Steinhoff, T., Sun, Q.,
1286 Sutton, A. J., Sweeney, C., Takao, S., Tanhua, T., Tans, P. P., Tian, X., Tian, H., Tilbrook, B., Tsujino, H.,
1287 Tubiello, F., van der Werf, G. R., Walker, A. P., Wanninkhof, R., Whitehead, C., Willstrand Wranne, A.,
1288 Wright, R., Yuan, W., Yue, C., Yue, X., Zaehle, S., Zeng, J., and Zheng, B.: Global Carbon Budget 2022, *Earth*
1289 *Syst. Sci. Data*, 14, 4811–4900, <https://doi.org/10.5194/essd-14-4811-2022>, 2022.
1290
1291 Friedlingstein, P., O'Sullivan, M., Jones, M. W., Andrew, R. M., Bakker, D. C. E., Hauck, J., Landschützer, P.,
1292 Le Quéré, C., Luijkx, I. T., Peters, G. P., Peters, W., Pongratz, J., Schwingshackl, C., Sitch, S., Canadell, J. G.,
1293 Ciais, P., Jackson, R. B., Alin, S. R., Anthoni, P., Barbero, L., Bates, N. R., Becker, M., Bellouin, N., Decharme,
1294 B., Bopp, L., Brasika, I. B. M., Cadule, P., Chamberlain, M. A., Chandra, N., Chau, T.-T.-T., Chevallier, F.,
1295 Chini, L. P., Cronin, M., Dou, X., Enyo, K., Evans, W., Falk, S., Feely, R. A., Feng, L., Ford, D. J., Gasser, T.,
1296 Ghattas, J., Gkritzalis, T., Grassi, G., Gregor, L., Gruber, N., Gürses, Ö., Harris, I., Hefner, M., Heinke, J.,
1297 Houghton, R. A., Hurtt, G. C., Iida, Y., Ilyina, T., Jacobson, A. R., Jain, A., Jarníková, T., Jersild, A., Jiang, F.,
1298 Jin, Z., Joos, F., Kato, E., Keeling, R. F., Kennedy, D., Klein Goldewijk, K., Knauer, J., Korsbakken, J. I.,
1299 Körtzinger, A., Lan, X., Lefèvre, N., Li, H., Liu, J., Liu, Z., Ma, L., Marland, G., Mayot, N., McGuire, P. C.,
1300 McKinley, G. A., Meyer, G., Morgan, E. J., Munro, D. R., Nakaoka, S.-I., Niwa, Y., O'Brien, K. M., Olsen, A.,
1301 Omar, A. M., Ono, T., Paulsen, M., Pierrot, D., Pocock, K., Poulter, B., Powis, C. M., Rehder, G., Resplandy, L.,
1302 Robertson, E., Rödenbeck, C., Rosan, T. M., Schwinger, J., Séférian, R., Smallman, T. L., Smith, S. M.,
1303 Sospedra-Alfonso, R., Sun, Q., Sutton, A. J., Sweeney, C., Takao, S., Tans, P. P., Tian, H., Tilbrook, B., Tsujino,
1304 H., Tubiello, F., van der Werf, G. R., van Ooijen, E., Wanninkhof, R., Watanabe, M., Wimart-Rousseau, C.,
1305 Yang, D., Yang, X., Yuan, W., Yue, X., Zaehle, S., Zeng, J., and Zheng, B.: Global Carbon Budget 2023, *Earth*
1306 *Syst. Sci. Data*, 15, 5301–5369, <https://doi.org/10.5194/essd-15-5301-2023>, 2023.
1307
1308 Fröb, F., Olsen, A., Becker, M., Chafik, L., Johannessen, T., Reverdin, G., and Omar, A.: Wintertime fCO₂
1309 variability in the subpolar North Atlantic since 2004. *Geophysical Research Letters*, 46,
1310 <https://doi.org/10.1029/2018GL080554>, 2019.
1311
1312 Gac, J.-P., Marrec, P., Cariou, T., Grosstefan, E., Macé, E., Rimmelin-Maury, P., Vernet, M., and Bozec, Y.:
1313 Decadal Dynamics of the CO₂ System and Associated Ocean Acidification in Coastal Ecosystems of the North
1314 East Atlantic Ocean. *Front. Mar. Sci.* 8:688008. doi:10.3389/fmars.2021.688008, 2021.
1315
1316 Gallego, M. A., Timmermann, A., Friedrich, T., and Zeebe, R. E.: Drivers of future seasonal cycle changes in
1317 oceanic pCO₂, *Biogeosciences*, 15, 5315–5327, <https://doi.org/10.5194/bg-15-5315-2018>, 2018.
1318
1319 Gattuso, J.-P., Magnan, A., Billé, R., Cheung, W. W. L., Howes, E. L., Joos, F., Allemand, D., Bopp, L., Cooley,
1320 S., Eakin, M., Hoegh-Guldberg, O., Kelly, R. P., Pörtner, H.-O., Rogers, A. D., Baxter, J. M., Laffoley, D.,
1321 Osborn, D., Rankovic, A., Rochette, J., Sumaila, U. R., Treyer, S., and Turley, C.: Contrasting futures for ocean

1322 and society from different anthropogenic CO₂ emissions scenarios. *Science* 349:aac4722.doi:
1323 10.1126/science.aac4722, 2015.

1324

1325 Gattuso, Jean-Pierre; Alliouane, Samir; Mousseau, Laure (2021): Seawater carbonate chemistry in the Bay of
1326 Villefranche, Point B (France), January 2007 - June 2023 [dataset]. PANGAEA,
1327 <https://doi.org/10.1594/PANGAEA.727120>

1328

1329 Gibb, O., Cyr, F., Azetsu-Scott, K., Chassé, J., Childs, D., Gabriel, C.-E., Galbraith, P. S., Maillet, G., Pepin, P.,
1330 Punshon, S., and Starr, M.: Spatiotemporal variability in pH and carbonate parameters on the Canadian Atlantic
1331 continental shelf between 2014 and 2022, *Earth Syst. Sci. Data*, 15, 4127–4162, <https://doi.org/10.5194/essd-15-4127-2023>, 2023.

1333

1334 Goyet, C., Beauverger, C., Brunet, C., and Poisson, A.: Distribution of carbon dioxide partial pressure in surface
1335 waters of the Southwest Indian Ocean, *Tellus B: Chemical and Physical Meteorology*, 43:1, 1-11, DOI:
1336 [10.3402/tellusb.v43i1.15242](https://doi.org/10.3402/tellusb.v43i1.15242), 1991.

1337

1338 Goyet C., Hassoun, A. E. R. Gemayel, E. Touratier, F., Abboud-Abi Saab M. and Guglielmi, V.:
1339 Thermodynamic forecasts of the Mediterranean Sea Acidification. *Mediterranean Marine Science*, 17/2, 508-
1340 518, <http://dx.doi.org/10.12681/mms.1487>, 2016

1341

1342 Goyet C., Benallal, M.A., Bijoux A., Guglielmi, V., Moussa, H., Ribou, A.-C., and Touratier, F.: Ch.39,
1343 Evolution of human Impact on Oceans: Tipping points of socio-ecological Coviability. In: Coviability of Social
1344 and Ecological Systems: Reconnecting Mankind to the Biosphere in an Era of Global Change. O.Barrière et al.
1345 (eds.) Springer International Publishing AG, part of Springer Nature 2019. https://doi.org/10.1007/978-3-319-78111-2_12, 2019

1347

1348 Gregor, L. and Gruber, N.: OceanSODA-ETHZ: a global gridded data set of the surface ocean carbonate system
1349 for seasonal to decadal studies of ocean acidification, *Earth Syst. Sci. Data*, 13, 777–808,
1350 <https://doi.org/10.5194/essd-13-777-2021>, 2021.

1351

1352 Gregor, L., Shutler, J., and Gruber, N.: High-resolution variability of the ocean carbon sink. *Global
1353 Biogeochemical Cycles*, 38, e2024GB008127. <https://doi.org/10.1029/2024GB008127>, 2024

1354

1355 Gruber, N., Clement, D. , Carter, B. R., Feely, R. A., van Heuven, S., Hoppema, M., Ishii, M., Key, R. M.,
1356 Kozyr, A., Lauvset, S. K., Lo Monaco, C. , Mathis, J. T., Murata, A., Olsen, A., Perez, F. F., Sabine, C. L.,
1357 Tanhua, T., and Wanninkhof, R.: The oceanic sink for anthropogenic CO₂ from 1994 to 2007, *Science* vol. 363
1358 (issue 6432), pp. 1193-1199. DOI: 10.1126/science.aau5153, 2019.

1359

1360 Guglielmi V., Touratier, F., and Goyet, C.: Design of sampling strategy measurements of CO₂/carbonate
1361 properties. *Journal of Oceanography and Aquaculture*, DOI: 10.23880/ijoac-16000227, 2022

1362

1363 Guglielmi V., Touratier, F., and Goyet, C.: Determination of discrete sampling locations minimizing both the
1364 number of samples and the maximum interpolation error: Application to measurements of carbonate chemistry in
1365 surface ocean, *Journal of Sea Research*, <https://doi.org/10.1016/j.seares.2023.102336>, 2023

1366

1367 Hauck, J., Gregor, L., Nissen, C., Patara, L., Hague, M., Mongwe, P., et al.: The Southern Ocean carbon cycle
1368 1985–2018: Mean, seasonal cycle, trends, and storage. *Global Biogeochemical Cycles*, 37, e2023GB007848.
1369 <https://doi.org/10.1029/2023GB007848>, 2023

1370

1371 Ho, D. T., Bopp, L., Palter, J. B., Long, M. C., Boyd, P.W., Neukermans, G., and Bach, L. T. : Monitoring,
1372 reporting, and verification for ocean alkalinity enhancement. *State of the Planet*, 2-oea2023, 1–12, 2023.

1373

- 1374 Holliday, N.P., Bersch, M., Berx, B., Chafik, L., Cunningham, S., Florindo-López, C., Hátún, H., Johns, W.,
1375 Josey, S.A., Larsen, K.M.H., Mulet, S., Oltmanns, M., Reverdin, G., Rossby, T., Thierry, V., Valdimarsson, H.,
1376 Yashayaev, I. : Ocean circulation causes the largest freshening event for 120 years in eastern subpolar North
1377 Atlantic. Nat. Commun., 11. <https://doi.org/10.1038/s41467-020-14474-y>, 2020
- 1378
- 1379 Howes, E., Stemmann, L., Assailly, C., Irisson, J.-O., Dima, M., Bijma, J., Gattuso, J.-P.: Pteropod time series
1380 from the North Western Mediterranean (1967-2003): impacts of pH and climate variability. Mar Ecol Prog Ser
1381 531: 193-206, doi: 10.3354/meps11322. 2015.
- 1382
- 1383 Huang, B., P. W. Thorne, V. F. Banzon, T. Boyer, G. Chepurin, J. H. Lawrimore, M. J. Menne, T. M. Smith, R.
1384 S. Vose, and H.-M. Zhang: Extended Reconstructed Sea Surface Temperature, version 5 (ERSSTv5): Upgrades,
1385 validations, and intercomparisons. J. Climate, 30, 8179-8205, doi:10.1175/JCLI-D-16-0836.1, 2017
- 1386
- 1387 IPCC. Changing Ocean, Marine Ecosystems, and Dependent Communities. in The Ocean and Cryosphere in a
1388 Changing Climate 447–588 (Cambridge University Press, 2022). doi:10.1017/9781009157964.007. 2022
- 1389
- 1390 Jiang, Z.-P., Tyrrell, T., Hydes, D. J., Dai, M., and Hartman, S. E.: Variability of alkalinity and the alkalinity-
1391 salinity relationship in the tropical and subtropical surface ocean, Global Biogeochem. Cycles, 28, 729–742,
1392 doi:10.1002/2013GB004678, 2014.
- 1393
- 1394 Jiang, L.-Q., Feely, R. A., Wanninkhof, R., Greeley, D., Barbero, L., Alin, S., Carter, B. R., Pierrot, D.,
1395 Featherstone, C., Hooper, J., Melrose, C., Monacci, N., Sharp, J. D., Shellito, S., Xu, Y.-Y., Kozyr, A., Byrne, R.
1396 H., Cai, W.-J., Cross, J., Johnson, G. C., Hales, B., Langdon, C., Mathis, J., Salisbury, J., and Townsend, D. W.:
1397 Coastal Ocean Data Analysis Product in North America (CODAP-NA) – an internally consistent data product for
1398 discrete inorganic carbon, oxygen, and nutrients on the North American ocean margins. Earth System Science
1399 Data, 13(6), 2777–2799. <https://doi.org/10.5194/essd-13-2777-2021>, 2021
- 1400
- 1401 Jiang, L.-Q., Dunne, J., Carter, B. R., Tjiputra, J. F., Terhaar, J., Sharp, J. D., et al.: Global surface ocean
1402 acidification indicators from 1750 to 2100. Journal of Advances in Modeling Earth Systems, 15,
1403 e2022MS003563. <https://doi.org/10.1029/2022MS003563>, 2023
- 1404
- 1405 Jiang, L.Q., Fay, A., Müller, J. D. et al: Synthesis products for ocean carbon chemistry. In prep., 2024.
- 1406
- 1407 Jing, Y., Li, Y., Xu, Y., and Fan, G.: Influences of the NAO on the North Atlantic CO₂ fluxes in winter and
1408 summer on the interannual scale. Advances in Atmospheric Sciences, 36(11), 1288–1298.
1409 <https://doi.org/10.1007/s00376-019-8247-2>, 2019
- 1410
- 1411 Kapsenberg, L., Alliouane, S., Gazeau, F., Mousseau, L., and Gattuso, J.-P.: Coastal ocean acidification and
1412 increasing total alkalinity in the northwestern Mediterranean Sea, Ocean Sci., 13, 411-426, doi:10.5194/os-13-
1413 411-2017, 2017.
- 1414
- 1415 Khatriwala, S., Tanhua, T., Mikaloff Fletcher, S., Gerber, M., Doney, S. C., Graven, H. D., Gruber, N.,
1416 McKinley, G. A., Murata, A., Ríos, A. F., and Sabine, C. L.: Global ocean storage of anthropogenic carbon,
1417 Biogeosciences, 10, 2169-2191, <https://doi.org/10.5194/bg-10-2169-2013>, 2013.
- 1418
- 1419 Koffi, U., Lefèvre, N., Kouadio, G., and Boutin, J.: Surface CO₂ parameters and air-sea CO₂ fluxes distribution
1420 in the eastern equatorial Altantic Ocean. J. Marine Systems, doi:10.1016/j.jmarsys/2010.04.010. 2010.
- 1421
- 1422 Kwiatkowski, L., Torres, O., Bopp, L., Aumont, O., Chamberlain, M., Christian, J. R., Dunne, J. P., Gehlen, M.,
1423 Ilyina, T., John, J. G., Lenton, A., Li, H., Lovenduski, N. S., Orr, J. C., Palmieri, J., Santana-Falcón, Y.,
1424 Schwinger, J., Séférian, R., Stock, C. A., Tagliabue, A., Takano, Y., Tjiputra, J., Toyama, K., Tsujino, H.,
1425 Watanabe, M., Yamamoto, A., Yool, A., and Ziehn, T.: Twenty-first century ocean warming, acidification,

1426 deoxygenation, and upper-ocean nutrient and primary production decline from CMIP6 model projections,
1427 Biogeosciences, 17, 3439–3470, <https://doi.org/10.5194/bg-17-3439-2020>, 2020.

1428

1429 Lacoue-Labarthe, T., Nunes, P. A. L. D., Ziveri, P., Cinar, M., Gazeau, F., Hall-Spencer, J. M., Hilmi, N.,
1430 Moschella, P., Safa, A., Sauzade, D., and Turley, C.: Impacts of ocean acidification in a warming Mediterranean
1431 Sea: An overview, Regional Studies in Marine Science, 5, 1–11, doi:10.1016/j.rsma.2015.12.005, 2016.

1432

1433 Lagoutte, E., A. Tribollet, S. Bureau, et al., Biogeochemical evidence of flow re-entrainment on the main
1434 fringing reef of La Reunion Island, Marine Chemistry, <https://doi.org/10.1016/j.marchem.2024.104352>, 2023.

1435

1436 Laika, H. E., Goyet C., Vouve F., Poisson A., and Touratier F. : Interannual properties of the CO₂ system in the
1437 Southern Ocean south of Australia. Antarctic Science, 21(6), 663-680.
1438 <https://doi.org/10.1017/S0954102009990319>, 2009

1439

1440 Lan, X., Tans, P. and K.W. Thoning: Trends in globally-averaged CO₂ determined from NOAA Global
1441 Monitoring Laboratory measurements. Version 2024-08 <https://doi.org/10.15138/9N0H-ZH07> (last access: 14
1442 August 2024), 2024.

1443

1444 Landschützer, P., Gruber, N., Bakker, D. C. E., Stemmler, I., and Six, K. D.: Strengthening seasonal marine CO₂
1445 variations due to increasing atmospheric CO₂. Nature Climate Change, 8(2), 146–150.
1446 <https://doi.org/10.1038/s41558-017-0057-x>, 2018

1447

1448 Landschützer, P., Ilyina, T., and Lovenduski, N. S. : Detecting regional modes of variability in observation-
1449 based surface ocean pCO₂. Geophysical Research Letters, 46. <https://doi.org/10.1029/2018GL081756>, 2019

1450

1451 Lange, N., Fiedler, B., Álvarez, M., Benoit-Cattin, A., Benway, H., Buttigieg, P. L., Coppola, L., Currie, K.,
1452 Flecha, S., Gerlach, D. S., Honda, M., Huertas, I. E., Lauvset, S. K., Muller-Karger, F., Körtzinger, A., O'Brien,
1453 K. M., Ólafsdóttir, S. R., Pacheco, F. C., Rueda-Roa, D., Skjelvan, I., Wakita, M., White, A., and Tanhua, T.:
1454 Synthesis Product for Ocean Time Series (SPOTS) – a ship-based biogeochemical pilot, Earth Syst. Sci. Data,
1455 16, 1901–1931, <https://doi.org/10.5194/essd-16-1901-2024>, 2024.

1456

1457 LANSARD Bruno (2014) DICASE cruise, RV Téthys II, <https://doi.org/10.17600/14007100>

1458

1459 Laruelle, G. G., Dürr, H. H., Lauerwald, R., Hartmann, J., Slomp, C. P., Goossens, N., and Regnier, P. A. G.:
1460 Global multi-scale segmentation of continental and coastal waters from the watersheds to the continental
1461 margins, Hydrol. Earth Syst. Sci., 17, 2029–2051, <https://doi.org/10.5194/hess-17-2029-2013>, 2013.

1462

1463 Laruelle, G. G. et al. Continental shelves as a variable but increasing global sink for atmospheric carbon dioxide.
1464 Nat.Commun. 9, 454, DOI: 10.1038/s41467-017-02738-z, 2018

1465

1466 Lauvset, S. K., Lange, N., Tanhua, T., Bittig, H. C., Olsen, A., Kozyr, A., Álvarez, M., Azetsu-Scott, K., Brown,
1467 P. J., Carter, B. R., Cotrim da Cunha, L., Hoppema, M., Humphreys, M. P., Ishii, M., Jeansson, E., Murata, A.,
1468 Müller, J. D., Pérez, F. F., Schirnick, C., Steinfeldt, R., Suzuki, T., Ulfsbo, A., Velo, A., Woosley, R. J., and
1469 Key, R. M.: The annual update GLODAPv2.2023: the global interior ocean biogeochemical data product, Earth
1470 Syst. Sci. Data, 16, 2047–2072, <https://doi.org/10.5194/essd-16-2047-2024>, 2024.

1471

1472 Lefèvre, D.: MOOSE (ANTARES), <https://doi.org/10.18142/233>, 2010.

1473

1474 Lefèvre N.: Carbon parameters along a zonal transect. SEANOE. <https://doi.org/10.17882/58575>, 2010.

1475

1476 Lefèvre Nathalie (2017). Carbon parameters in the gulf of Maranhao. SEANOE. <https://doi.org/10.17882/62417>

1477

- 1478 Lefèvre Nathalie (2018). Carbon parameters in the Western tropical Atlantic. SEANOE.
1479 <https://doi.org/10.17882/58406>
- 1480
- 1481 Lefèvre Nathalie (2019). Carbon parameters in the Eastern Tropical Atlantic in 2019. SEANOE.
1482 <https://doi.org/10.17882/83682>
- 1483
- 1484 Lefèvre Nathalie (2020). Inorganic carbon and alkalinity in the Eastern tropical Atlantic measured during the
1485 PIRATA FR-30 cruise in February-March 2020. SEANOE. <https://doi.org/10.17882/90742>
- 1486
- 1487 Lefèvre Nathalie (2022). Inorganic carbon and alkalinity in the Eastern tropical Atlantic in 2022. SEANOE.
1488 <https://doi.org/10.17882/92386>
- 1489
- 1490 Lefèvre, N., Urbano, D.F., Gallois, F., and Diverrès, D.: Impact of physical processes on the seasonal
1491 distribution of CO₂ in the western tropical Atlantic. *Journal of Geophysical Research* 119,
1492 doi: 10.1002/2013JC009248. doi: DOI: 10.1002/2013JC009248, 2014
- 1493
- 1494 Lefèvre, N., Veleda, D., Araujo, M., Caniaux, G.: Variability and trends of carbon parameters at a time series in
1495 the eastern tropical Atlantic. *Tellus B*, Co-Action Publishing, 68, pp.30305. 10.3402/tellusb.v68.30305. 2016.
- 1496
- 1497 Lefèvre N., da Silva Dias F. J., de Torres A. R., Noriega C., Araujo M., de Castro A. C. L., Rocha C., Jiang S.,
1498 Ibánhez J. S. P.: A source of CO₂ to the atmosphere throughout the year in the Maranhense continental shelf
1499 (2°30'S, Brazil). *Continental Shelf Research*, 141, 38-50. <https://doi.org/10.1016/j.csr.2017.05.004>, 2017a
- 1500
- 1501 Lefèvre N., Flores Montes M., Gaspar F. L., Rocha C., Jiang S., De Araújo M. C., Ibánhez J. S. P.: Net
1502 Heterotrophy in the Amazon Continental Shelf Changes Rapidly to a Sink of CO₂ in the Outer Amazon Plume.
1503 *Frontiers in Marine Science*, 4, -. <https://doi.org/10.3389/fmars.2017.00278>, 2017b
- 1504
- 1505 Lefèvre, N., Mejia, C., Khvorostyanov, D., Beaumont, L., and Koffi, U.: Ocean Circulation Drives the
1506 Variability of the Carbon System in the Eastern Tropical Atlantic. *Oceans*, 2021, 2, 126–148.
1507 <https://doi.org/10.3390/oceans2010008>, 2021.
- 1508
- 1509 Lefèvre, N., Veleda, D., Hartman, S.E.: Outgassing of CO₂ dominates in the coastal upwelling off the northwest
1510 African coast, *Deep-Sea Research Part I*, doi: <https://doi.org/10.1016/j.dsr.2023.104130>, 2023
- 1511
- 1512 Lefèvre, N., Veleda, D. and Beaumont; L.: Trends and drivers of CO₂ parameters, from 2006 to 2021, at a time-
1513 series station in the Eastern Tropical Atlantic (6°S, 10°W). *Front. Mar. Sci.* 11:1299071. doi:
1514 10.3389/fmars.2024.1299071, 2024
- 1515
- 1516 Leseurre, C.: Mécanismes de contrôle de l'absorption de CO₂ anthropique et de l'acidification des eaux dans les
1517 océans Atlantique Nord et Austral. PhD Thesis, Sorbonne Univ., 270 pp. <https://theses.hal.science/tel-04028410>,
1518 2022
- 1519
- 1520 Leseurre, C., Lo Monaco, C., Reverdin, G., Metzl, N., Fin, J., Olafsdottir, S., and Racapé, V.: Ocean carbonate
1521 system variability in the North Atlantic Subpolar surface water (1993–2017), *Biogeosciences*, 17, 2553–2577,
1522 <https://doi.org/10.5194/bg-17-2553-2020>, 2020
- 1523
- 1524 Leseurre, C., Lo Monaco, C., Reverdin, G., Metzl, N., Fin, J., Mignon, C., and Benito, L.: Summer trends and
1525 drivers of sea surface fCO₂ and pH changes observed in the southern Indian Ocean over the last two decades
1526 (1998–2019), *Biogeosciences*, 19, 2599–2625, <https://doi.org/10.5194/bg-19-2599-2022>, 2022.
- 1527
- 1528 Li, X., et al.: The source and accumulation of anthropogenic carbon in the U.S. East Coast, *Sci. Adv.* 10,
1529 eadl3169, DOI: 10.1126/sciadv.adl3169, 2024
- 1530

- 1531 LO MONACO Claire, METZL Nicolas (2019) VT 163 / OISO-29 cruise, RV Marion Dufresne,
1532 <https://doi.org/10.17600/18000972>
- 1533
- 1534 LO MONACO Claire (2020) OISO-30 cruise, RV Marion Dufresne, <https://doi.org/10.17600/18000679>
- 1535
- 1536 LO MONACO Claire, JEANDEL Catherine, PLANQUETTE Hélène (2021) OISO-31 cruise, RV Marion
1537 Dufresne, <https://doi.org/10.17600/18001254>
- 1538
- 1539 Lo Monaco, Claire; Metzl, Nicolas; Fin, Jonathan (2022). Sea surface measurements of dissolved inorganic
1540 carbon (DIC), total alkalinity (TALK), temperature and salinity during the R/V Marion-Dufresne Ocean Indien
1541 Service d'Observations - 29 (OISO-29) cruise (EXPOCODE 35MV20190106) in the Indian Ocean from 2019-
1542 01-06 to 2019-02-09 (NCEI Accession 0252612). NOAA National Centers for Environmental Information.
1543 Dataset. <https://doi.org/10.25921/8ajx-za24>. Accessed 14-Aug-2024.
- 1544
- 1545 Lo Monaco, Claire; Metzl, Nicolas (2023). Sea surface measurements of dissolved inorganic carbon (DIC), total
1546 alkalinity (TALK), temperature and salinity during the R/V Marion-Dufresne Ocean Indien Service
1547 d'Observations - 30 (OISO-30) cruise (EXPOCODE 35MV20200106) in the Indian Ocean from 2020-01-06 to
1548 2020-02-01 (NCEI Accession 0280937). NOAA National Centers for Environmental Information. Dataset.
1549 <https://doi.org/10.25921/n2g0-pp38>. Accessed 14-Aug-2024
- 1550
- 1551 Lo Monaco, Claire; Metzl, Nicolas; Fin, Jonathan (2023). Sea surface measurements of dissolved inorganic
1552 carbon (DIC), total alkalinity (TALK), temperature and salinity during the R/V Marion-Dufresne Ocean
1553 Indien Service d'Observations - 31 (OISO-31) cruise (EXPOCODE 35MV20210113) in the Indian Ocean
1554 from 2021-01-14 to 2021-03-04 (NCEI Accession 0280946). NOAA National Centers for Environmental
1555 Information. Dataset. <https://doi.org/10.25921/7sb2-k852>. Accessed 14-Aug-2024
- 1556
- 1557 Mathis, M., Lacroix, F., Hagemann, S. et al.: Enhanced CO₂ uptake of the coastal ocean is dominated by
1558 biological carbon fixation. Nat. Clim. Chang.. <https://doi.org/10.1038/s41558-024-01956-w>, 2024
- 1559
- 1560 Maugendre, L., J.-P. Gattuso, J. Louis, A. de Kluijver, S. Marro, K. Soetaert, F. Gazeau: Effect of ocean
1561 warming and acidification on a plankton community in the NW Mediterranean Sea, ICES Journal of Marine
1562 Science, Volume 72, Issue 6, July/August 2015, Pages 1744–1755, <https://doi.org/10.1093/icesjms/fsu161>, 2015
- 1563
- 1564 Mercier, H., Lherminier, P., Sarafanov, A., Gaillard, F., Daniault, N., Desbruyères, D., Falina, A., Ferron, B.,
1565 Huck, T., and Thierry, V.: Variability of the meridional overturning circulation at the Greenland-Portugal Ovide
1566 section from 1993 to 2010. Progress in Oceanography, 132, 250-261, [doi:10.1016/j.pocean.2013.11.001](https://doi.org/10.1016/j.pocean.2013.11.001), 2015
- 1567
- 1568 Mercier, H., Desbruyères, D., Lherminier, P., Velo, A., Carracedo, L., Fontela, M., and Pérez, F. F.: New
1569 insights into the eastern subpolar North Atlantic meridional overturning circulation from OVIDE, Ocean Sci.,
1570 20, 779–797, <https://doi.org/10.5194/os-20-779-2024>, 2024.
- 1571
- 1572 Metzl, N., Brunet, C., Jabaud-Jan, A., Poisson, A., and Schauer, B.: Summer and winter air-sea CO₂ fluxes in
1573 the Southern Ocean *Deep Sea Res I*, 53, 1548-1563, doi:10.1016/j.dsr.2006.07.006. 2006.
- 1574
- 1575 Metzl, N., Corbière, A., Reverdin, G., Lenton, A., Takahashi, T., Olsen, A., Johannessen, T., Pierrot, D.,
1576 Wanninkhof, R., Ólafsdóttir, S. R., Olafsson, J., and Ramonet, M.: Recent acceleration of the sea surface fCO₂
1577 growth rate in the North Atlantic subpolar gyre (1993-2008) revealed by winter observations, Global
1578 Biogeochem. Cycles, 24, GB4004, doi:10.1029/2009GB003658, 2010.
- 1579
- 1580 Metzl, N., and Lo Monaco, C.: OISO - OCÉAN INDIEN SERVICE D'OBSERVATION,
1581 <https://doi.org/10.18142/228>, 1998.
- 1582

- 1583 Metzl, N., Lo Monaco, C., Leseurre, C., Ridame, C., Fin, J., Mignon, C., Gehlen, M., and Chau, T. T. T.: The
1584 impact of the South-East Madagascar Bloom on the oceanic CO₂ sink, *Biogeosciences*, 19, 1451–1468,
1585 <https://doi.org/10.5194/bg-19-1451-2022>, 2022
- 1586
- 1587 Metzl Nicolas, Fin Jonathan, Lo Monaco Claire, Mignon Claude, Alliouane Samir, Antoine David, Bourdin
1588 Guillaume, Boutin Jacqueline, Bozec Yann, Conan Pascal, Coppola Laurent, Douville Eric, Durrieu de Madron
1589 Xavier, Gattuso Jean-Pierre, Gazeau Frédéric, Golbol Melek, Lansard Bruno, Lefèvre Dominique, Lefèvre
1590 Nathalie, Lombard Fabien, Louanchi Férial, Merlivat Liliane, Olivier Léa, Petrenko Anne, Petton Sébastien,
1591 Pujo-Pay Mireille, Rabouille Christophe, Reverdin Gilles, Ridame Céline, Tribollet Aline, Vellucci Vincenzo,
1592 Wagener Thibaut, Wimart-Rousseau Cathy: SNAPO-CO₂ data-set: A synthesis of total alkalinity and total
1593 dissolved inorganic carbon observations in the global ocean (1993–2022). SEANOE.
1594 <https://doi.org/10.17882/95414>, 2023
- 1595
- 1596 Metzl, N., Fin, J., Lo Monaco, C., Mignon, C., Alliouane, S., Antoine, D., Bourdin, G., Boutin, J., Bozec, Y.,
1597 Conan, P., Coppola, L., Diaz, F., Douville, E., Durrieu de Madron, X., Gattuso, J.-P., Gazeau, F., Golbol, M.,
1598 Lansard, B., Lefèvre, D., Lefèvre, N., Lombard, F., Louanchi, F., Merlivat, L., Olivier, L., Petrenko, A., Petton,
1599 S., Pujo-Pay, M., Rabouille, C., Reverdin, G., Ridame, C., Tribollet, A., Vellucci, V., Wagener, T., and Wimart-
1600 Rousseau, C.: A synthesis of ocean total alkalinity and dissolved inorganic carbon measurements from 1993 to
1601 2022: the SNAPO-CO₂-v1 dataset, *Earth Syst. Sci. Data*, 16, 89–120, <https://doi.org/10.5194/essd-16-89-2024>,
1602 2024a
- 1603
- 1604 Metzl, N., Lo Monaco, C., Leseurre, C., Ridame, C., Reverdin, G., Chau, T. T. T., Chevallier, F., and Gehlen,
1605 M.: Anthropogenic CO₂, air-sea CO₂ fluxes, and acidification in the Southern Ocean: results from a time-series
1606 analysis at station OISO-KERFIX (51° S–68° E), *Ocean Sci.*, 20, 725–758, <https://doi.org/10.5194/os-20-725-2024>, 2024b.
- 1608
- 1609 Metzl, N., Lo Monaco, C., Barut, G., and Ternon, J.-F.: Contrasting trends of the ocean CO₂ sink and pH in the
1610 Agulhas current system and the Mozambique Basin, South-Western Indian Ocean (1963–2023). *Deep Sea Res.*,
1611 special issue IIOE-2, in rev., 2024c
- 1612
- 1613 Metzl Nicolas, Fin Jonathan, Lo Monaco Claire, Mignon Claude, Alliouane Samir, Bombled Bruno, Boutin
1614 Jacqueline, Bozec Yann, Comeau Steeve, Conan Pascal, Coppola Laurent, Cuet Pascale, Ferreira Eva, Gattuso
1615 Jean-Pierre, Gazeau Frédéric, Goyet Catherine, Grossteffan Emilie, Lansard Bruno, Lefèvre Dominique, Lefèvre
1616 Nathalie, Leseurre Coraline, Lombard Fabien, Petton Sébastien, Pujo-Pay Mireille, Rabouille Christophe,
1617 Reverdin Gilles, Ridame Céline, Rimmelin-Maury Peggy, Ternon Jean-François, Touratier Franck, Tribollet
1618 Aline, Wagener Thibaut, Wimart-Rousseau Cathy: An updated synthesis of ocean total alkalinity and dissolved
1619 inorganic carbon measurements from 1993 to 2023: the SNAPO-CO₂-v2 dataset. SEANOE.
1620 <https://doi.org/10.17882/102337>, 2024d
- 1621
- 1622 MICHEL Elisabeth, VIVIER Frédéric: STEP 2016 cruise, RV L'Atalante, <https://doi.org/10.17600/16000900>,
1623 2016
- 1624
- 1625 Mu, L., Gomes, H. do R., Burns, S. M., Goes, J. I., Coles, V. J., Rezende, C. E., et al.: Temporal Variability of
1626 Air-Sea CO₂ flux in the Western Tropical North Atlantic Influenced by the Amazon River Plume. *Global
1627 Biogeochemical Cycles*, 35(6). <https://doi.org/10.1029/2020GB006798>, 2021
- 1628
- 1629 Munro, D. R., Lovenduski, N. S., Takahashi, T., Stephens, B. B., Newberger, T., and Sweeney, C.: Recent
1630 evidence for a strengthening CO₂ sink in the Southern Ocean from carbonate system measurements in the Drake
1631 Passage (2002–2015), *Geophys. Res. Lett.*, 42, 7623–7630, <https://doi.org/10.1002/2015GL065194>, 2015.
- 1632
- 1633 Müller, J. D., Gruber, N., Carter, B., Feely, R., Ishii, M., Lange, N., et al.: Decadal trends in the oceanic storage
1634 of anthropogenic carbon from 1994 to 2014. *AGU Advances*, 4, e2023AV000875.
1635 <https://doi.org/10.1029/2023AV000875>, 2023

- 1636
1637 Newton, J.A., Feely, R. A., Jewett, E. B., Williamson, P. and Mathis, J.: Global Ocean Acidification Observing
1638 Network: Requirements and Governance Plan. Second Edition, GOA-ON,
1639 <https://www.iaea.org/sites/default/files/18/06/goa-on-second-edition-2015.pdf>, 2015.
1640
1641 Olafsson, J., Olafsdottir, S. R., Benoit-Cattin, A., and Takahashi, T.: The Irminger Sea and the Iceland Sea time
1642 series measurements of sea water carbon and nutrient chemistry 1983–2008, *Earth Syst. Sci. Data*, 2, 99–104,
1643 <https://doi.org/10.5194/essd-2-99-2010>, 2010.
1644
1645 Olivier, L., Boutin, J., Reverdin, G., Lefèvre, N., Landschützer, P., Speich, S., Karstensen, J., Labaste, M.,
1646 Noisel, C., Ritschel, M., Steinhoff, T., and Wanninkhof, R.: Wintertime process study of the North Brazil
1647 Current rings reveals the region as a larger sink for CO₂ than expected, *Biogeosciences*, 19, 2969–2988,
1648 <https://doi.org/10.5194/bg-19-2969-2022>, 2022.
1649
1650 Olsen, A., Key, R. M., van Heuven, S., Lauvset, S. K., Velo, A., Lin, X., Schirnick, C., Kozyr, A., Tanhua, T.,
1651 Hoppema, M., Jutterström, S., Steinfeldt, R., Jeansson, E., Ishii, M., Pérez, F. F., and Suzuki, T.: The Global
1652 Ocean Data Analysis Project version 2 (GLODAPv2) – an internally consistent data product for the world ocean,
1653 *Earth Syst. Sci. Data*, 8, 297–323, <https://doi.org/10.5194/essd-8-297-2016>, 2016.
1654
1655 Oudot, C., Ternon, J. F., and Lecomte, J.: Measurements of atmospheric and oceanic CO₂ in the tropical Atlantic:
1656 10 years after the 1982–1984 FOCAL cruises. *Tellus B: Chemical and Physical Meteorology*, 47(1–2), 70–85.
<https://doi.org/10.3402/tellusb.v47i1-2.16032>, 1995
1658
1659 Padín, X. A., Velo, A., and Pérez, F. F.: ARIOS: a database for ocean acidification assessment in the Iberian
1660 upwelling system (1976–2018), *Earth Syst. Sci. Data*, 12, 2647–2663, <https://doi.org/10.5194/essd-12-2647-2020>, 2020.
1662
1663 Palacio-Castro, A. M., Enochs, I. C., Besemer, N., Boyd, A., Jankulak, M., Kolodziej, G., et al.: Coral reef
1664 carbonate chemistry reveals interannual, seasonal, and spatial impacts on ocean acidification off Florida. *Global
1665 Biogeochemical Cycles*, 37, e2023GB007789. <https://doi.org/10.1029/2023GB007789>, 2023
1666
1667 Pardo, P. C., Tilbrook, B., Langlais, C., Trull, T. W., and Rintoul, S. R.: Carbon uptake and biogeochemical
1668 change in the Southern Ocean, south of Tasmania. *Biogeosciences*, 14(22), 5217–5237.
1669 <https://doi.org/10.5194/bg-14-5217-2017>, 2017.
1670
1671 Pérez, F. F., Becker, M., Goris, N., Gehlen, M., López-Mozos, M., Tjiputra, J., et al.: An assessment of CO₂
1672 storage and sea-air fluxes for the Atlantic Ocean and Mediterranean Sea between 1985 and 2018. *Global
1673 Biogeochemical Cycles*, 38, e2023GB007862. <https://doi.org/10.1029/2023GB007862>, 2024
1674
1675 Petton, S., Pernet, F., Le Roy, V., Huber, M., Martin, S., Macé, É., Bozec, Y., Loisel, S., Rimmelin Maury, P.,
1676 Grossteffan, É., Repecaud, M., Quemener, L., Retho, M., Manac'h, S., Papin, M., Pineau, P., Lacoue-Labarthe,
1677 T., Deborde, J., Costes, L., Polsenaere, P., Rigouin, L., Benhamou, J., Gouriou, L., Lequeux, J., Labourdette, N.,
1678 Savoye, N., Messiaen, G., Foucault, E., Ouisse, V., Richard, M., Lagarde, F., Voron, F., Kempf, V., Mas, S.,
1679 Giannecchini, L., Vidussi, F., Mostajir, B., Leredde, Y., Alliouane, S., Gattuso, J.-P., and Gazeau, F.: French
1680 coastal network for carbonate system monitoring: the CocoriCO₂ dataset, *Earth Syst. Sci. Data*, 16, 1667–1688,
1681 <https://doi.org/10.5194/essd-16-1667-2024>, 2024.
1682
1683 Petton Sébastien, Pernet Fabrice, Le Roy Valerian, Huber Matthias, Martin Sophie, Mace Eric, Bozec Yann,
1684 Loisel Stéphane, Rimmelin-Maury Peggy, Grossteffan Emilie, Repecaud Michel, Quéméner Loïc, Retho
1685 Michael, Manach Soazig, Papin Mathias, Pineau Philippe, Lacoue-Labarthe Thomas, Deborde Jonathan, Costes
1686 Louis, Polsenaere Pierre, Rigouin Loic, Benhamou Jeremy, Gouriou Laure, Lequeux Joséphine, Labourdette
1687 Nathalie, Savoye Nicolas, Messiaen Gregory, Foucault Elodie, Lagarde Franck, Richard Marion, Ouisse
1688 Vincent, Voron Florian, Mas Sébastien, Giannecchini Léa, Vidussi Francesca, Mostajir Behzad, Leredde Yann,

- 1689 Kempf Valentin, Alliouane Samir, Gattuso Jean-Pierre, Gazeau Frédéric: French coastal carbonate dataset from
1690 the CocoriCO₂ project. SEANOE. <https://doi.org/10.17882/96982>, 2023
- 1691
- 1692 Poisson, A., Culkin, F., and Ridout, P.: Intercomparison of CO₂ measurements. Deep Sea Research Part A.
1693 Oceanographic Research Papers, 37, 10, 1647-1650, [https://doi.org/10.1016/0198-0149\(90\)90067-6](https://doi.org/10.1016/0198-0149(90)90067-6), 1990.
- 1694
- 1695 Pozzato, L., Rassmann, J., Lansard, B., Dumoulin, J.-P., Van Breugel, P., and Rabouille, C.: Origin of
1696 remineralized organic matter in sediments from the Rhone River prodelta (NW Mediterranean) traced by Delta
1697 C-14 and delta C-13 signatures of pore water DIC. Progress In Oceanography, 163, 112-122.
1698 <https://doi.org/10.1016/j.pocean.2017.05.008>, 2018
- 1699
- 1700 RABOUILLE Christophe (2010) MESURHOBENT 1 cruise, RV Téthys II, <https://doi.org/10.17600/10450020>
- 1701
- 1702 RABOUILLE Christophe (2013) CARBODELTA cruise, RV Téthys II, <https://doi.org/10.17600/13450060>
- 1703
- 1704 RABOUILLE Christophe (2018) MISSRHODIA2 cruise, RV Téthys II, <https://doi.org/10.17600/18000473>
- 1705
- 1706 RABOUILLE Christophe, BOURRIN François, BASSETTI Maria-Angela (2022) DELTARHONE-1 cruise, RV
1707 Téthys II, <https://doi.org/10.17600/18002027>
- 1708
- 1709 Regnier, P., Friedlingstein, P., Ciais, P., Mackenzie, F. T., Gruber, N., et al: Anthropogenic perturbation of the
1710 carbon fluxes from land to ocean. Nat. Geosci. 6:597–607, 2013.
- 1711
- 1712 Resplandy, L., Hogikyan, A., Müller, J. D., Najjar, R. G., Bange, H. W., Bianchi, D., et al.: A synthesis of global
1713 coastal ocean greenhouse gas fluxes. Global Biogeochemical Cycles, 38, e2023GB007803.
1714 <https://doi.org/10.1029/2023GB007803>, 2024
- 1715
- 1716 Revelle, R., and Suess, H. E.: Carbon dioxide exchange between atmosphere and ocean and the question of an
1717 increase of atmospheric CO₂ during the past decades. Tellus 9, 18–27. doi:10.1111/j.2153-
1718 3490.1957.tb01849.x., 1957.
- 1719
- 1720 Reverdin, G., Metzl, N., Olafsdottir, S., Racapé, V., Takahashi, T., Benetti, M., Valdimarsson, H., Benoit-Cattin,
1721 A., Danielsen, M., Fin, J., Naamar, A., Pierrot, D., Sullivan, K., Bringas, F., and Goni, G.: SURATLANT: a
1722 1993–2017 surface sampling in the central part of the North Atlantic subpolar gyre, Earth Syst. Sci. Data, 10,
1723 1901-1924, <https://doi.org/10.5194/essd-10-1901-2018>, 2018.
- 1724
- 1725 Reverdin, G., Metzl, N., Olafsdottir, S., Racapé, V., Takahashi, T., Benetti, M., Valdimarsson, H., Quay, P. D.,
1726 Benoit-Cattin, A., Danielsen, M., Fin, J., Naamar, A., Pierrot, D., Sullivan, K., Bringas, F., Goni, G., Becker M.,
1727 Leseurre C., and Olsen A.: SURATLANT: a surface dataset in the central part of the North Atlantic subpolar
1728 gyre. SEANOE. <https://doi.org/10.17882/54517>, 2023.
- 1729
- 1730 Rodgers, K. B., Schwinger, J., Fassbender, A. J., Landschützer, P., Yamaguchi, R., Frenzel, H., et al.: Seasonal
1731 variability of the surface ocean carbon cycle: A synthesis. Global Biogeochemical Cycles, 37, e2023GB007798.
1732 <https://doi.org/10.1029/2023GB007798>, 2023
- 1733
- 1734 Roobaert, A., Resplandy, L., Laruelle, G. G., Liao, E., and Regnier, P. : Unraveling the physical and biological
1735 controls of the global coastal CO₂ sink. Global Biogeochemical Cycles, 38, e2023GB007799.
1736 <https://doi.org/10.1029/2023GB007799>, 2024a
- 1737
- 1738 Roobaert, A., Regnier, P., Landschützer, P., and Laruelle, G. G.: A novel sea surface pCO₂-product for the
1739 global coastal ocean resolving trends over 1982–2020, Earth Syst. Sci. Data, 16, 421–441,
1740 <https://doi.org/10.5194/essd-16-421-2024>, 2024b.
- 1741

- 1742 Sarma, V. V. S. S., Krishna, M. S., Paul, Y. S., and Murty, V. S. N.: Observed changes in ocean acidity and
1743 carbon dioxide exchange in the coastal bay of Bengal—A link to air pollution. Tellus B: Chemical and Physical
1744 Meteorology, 67(1), 24638. <https://doi.org/10.3402/tellusb.v67.24638>, 2015
- 1745
- 1746 Sarma, V. V. S. S., Sridevi, B., Metzl, N., Patra, P. K., Lachkar, Z., Chakraborty, K., et al. : Air-sea fluxes of
1747 CO₂ in the Indian Ocean between 1985 and 2018: A synthesis based on observation-based surface CO₂, hindcast
1748 and atmospheric inversion models. Global Biogeochemical Cycles, 37, e2023GB007694.
1749 <https://doi.org/10.1029/2023GB007694>, 2023
- 1750
- 1751 Sarmiento, J.L., Johnson, K.S., Arteaga, L.A., Bushinsky, S.M., Cullen, H.M., Gray, A.R., Hotinski, R.M.,
1752 Maurer, T.L., Mazloff, M.R., Riser, S.C., Russell, J.L., Schofield, O.M., Talley, L.D., The Southern Ocean
1753 Carbon and Climate Observations and Modeling (SOCCOM) project: A review, Progress in Oceanography, doi:
1754 <https://doi.org/10.1016/j.pocean.2023.103130>, 2023
- 1755
- 1756 Schlitzer, R.: Ocean Data View, Ocean Data View, <http://odv.awi.de> (last access: 13 March 2019), 2018.
- 1757
- 1758 Schneider, A., Wallace, D. W. R., and Kötzinger, A.: Alkalinity of the Mediterranean Sea, Geophys. Res. Lett.,
1759 34, L15608, doi:10.1029/2006GL028842, 2007.
- 1760
- 1761 Schuster, U., McKinley, G. A., Bates, N., Chevallier, F., Doney, S. C., Fay, A. R., González-Dávila, M., Gruber,
1762 N., Jones, S., Krijnen, J., Landschützer, P., Lefèvre, N., Manizza, M., Mathis, J., Metzl, N., Olsen, A., Rios, A.
1763 F., Rödenbeck, C., Santana-Casiano, J. M., Takahashi, T., Wanninkhof, R., and Watson, A. J.: An assessment of
1764 the Atlantic and Arctic sea-air CO₂ fluxes, 1990–2009, Biogeosciences, 10, 607–627,
1765 <https://doi.org/10.5194/bg-10-607-2013>, 2013.
- 1766
- 1767 Shadwick, E., Rintoul, S., Tilbrook, B., Williams, G., Young, N., Fraser, A. D., et al.: Glacier tongue calving
1768 reduced dense water formation and enhanced carbon uptake. Geophysical Research Letters, 40(5), 904–909.
1769 <https://doi.org/10.1002/grl.50178>, 2013
- 1770
- 1771 Shadwick, E. H., B. Tilbrook, and G. D. Williams: Carbonate chemistry in the Mertz Polynya (East Antarctica):
1772 Biological and physical modification of dense water outflows and the export of anthropogenic CO₂, J. Geophys.
1773 Res. Oceans, 119, 1–14, doi:10.1002/2013JC009286, 2014
- 1774
- 1775 Shadwick, E. H., T. W. Trull, B. Tilbrook, A. J. Sutton, E. Schulz, and C. L. Sabine: Seasonality of biological
1776 and physical controls on surface ocean CO₂ from hourly observations at the Southern Ocean Time Series site
1777 south of Australia, Global Biogeochem. Cycles, 29, 223–238, doi:10.1002/2014GB004906, 2015
- 1778
- 1779 Shadwick, E. H., Wynn-Edwards, C. A., Matear, R. J., Jansen, P., Schulz, E. and Sutton, A. J.: Observed
1780 amplification of the seasonal CO₂ cycle at the Southern Ocean Time Series. Front. Mar. Sci. 10:1281854. doi:
1781 10.3389/fmars.2023.1281854, 2023
- 1782
- 1783 Siddiqui, A. H., Haine, T. W. N., Nguyen, A. T., and Buckley, M. W.: Controls on upper ocean salinity
1784 variability in the eastern subpolar North Atlantic during 1992–2017. Journal of Geophysical
1785 Research: Oceans, 129, e2024JC020887. <https://doi.org/10.1029/2024JC020887>, 2024
- 1786
- 1787 Sridevi, B., and Sarma, V. V. S. S.: Role of river discharge and warming on ocean acidification and pco₂ levels
1788 in the Bay of Bengal. Tellus B: Chemical and Physical Meteorology, 73 (1), 1–20., DOI:
1789 10.1080/16000889.2021.1971924, 2021
- 1790
- 1791 Sutton, A.J., Battisti, R., Carter, B., Evans, W., Newton, J., Alin, S., Bates, N.R., Cai, W.-J., Currie, K., Feely,
1792 R.A., Sabine, C., Tanhua, T., Tilbrook, B., and Wanninkhof, R.: Advancing best practices for assessing trends
1793 of ocean acidification time series. Frontiers in Marine Science, 9: 1045667. doi: 10.3389/fmars.2022.1045667,
1794 2022

- 1795
1796 Takahashi, T., Sutherland, S. C., Wanninkhof, R., Sweeney, C., Feely, R. A., Chipman, D. W., Hales, B.,
1797 Friederich, G., Chavez, F., Sabine, C., Watson, A. J., Bakker, D. C., Schuster, U., Metzl, N., Yoshikawa-Inoue,
1798 H., Ishii, M., Midorikawa, T., Nojiri, Y., Körtzinger, A., Steinhoff, T., Hoppema, M., Olafsson, J., Arnarson, T.
1799 S., Tilbrook, B., Johannessen, T., Olsen, A., Bellerby, R., Wong, C., Delille, B., Bates, N., and de Baar, H. J.:
1800 Climatological mean and decadal change in surface ocean pCO₂, and net sea air CO₂ flux over the global
1801 oceans. Deep-Sea Res. II, 56 (8-10), 554–577, <http://dx.doi.org/10.1016/j.dsr2.2008.12.009>. 2009.
1802
1803 Takahashi, T., Sutherland, S. C., Chipman, D. W., Goddard, J. G., Ho, C., Newberger, T., Sweeney, C. and
1804 Munro, D. R.: Climatological distributions of pH, pCO₂, total CO₂, alkalinity, and CaCO₃ saturation in the
1805 global surface ocean, and temporal changes at selected locations. Marine Chemistry, 164, 95–125,
1806 doi:10.1016/j.marchem.2014.06.004. 2014.
1807
1808 Ternon, J.-F., Oudot, C., Dessier, A., Diverres, D.: A seasonal tropical sink for atmospheric CO₂ in the Atlantic
1809 ocean: the role of the Amazon River discharge, Marine Chemistry, Volume 68, Issue 3, Pages 183-201,
1810 [https://doi.org/10.1016/S0304-4203\(99\)00077-8](https://doi.org/10.1016/S0304-4203(99)00077-8), 2000
1811
1812 TESTOR Pierre, COPPOLA Laurent, BOSSE Anthony (2021) MOOSE-GE 2021 cruise, RV Thalassa,
1813 <https://doi.org/10.17600/18001333>
1814
1815 TESTOR Pierre, COPPOLA Laurent, BOSSE Anthony (2022) MOOSE-GE 2022 cruise, RV Pourquoi pas ?,
1816 <https://doi.org/10.17600/18001854>
1817
1818 TESTOR Pierre, DURRIEU de MADRON Xavier (2023) MOOSE-GE 2023 cruise, RV Thalassa,
1819 <https://doi.org/10.17600/18002686>
1820
1821 Thomas, H., Prowe, A. E. F., Lima, I. D., Doney, S. C., Wanninkhof, R., Greatbatch, R. J., Schuster, U. and
1822 Corbière, A.: Changes in the North Atlantic Oscillation influence CO₂ uptake in the North Atlantic over the past
1823 2 decades, Global Biogeochemical Cycles, 22(4), doi:10.1029/2007GB003167, 2008
1824
1825 Tilbrook, B., Jewett, E. B., DeGrandpre, M. D., Hernandez-Ayon, J. M., Feely, R. A., Gledhill, D. K., Hansson,
1826 L., Isensee, K., Kurz, M. L., Newton, J. A., Siedlecki, S. A., Chai, F., Dupont, S., Graco, M., Calvo, E., Greeley,
1827 D., Kapsenberg, L., Lebrec, M., Pelejero, C., Schoo, K. L., and Telszewski, M.: An Enhanced Ocean
1828 Acidification Observing Network: From People to Technology to Data Synthesis and Information Exchange.
1829 *Frontiers in Marine Science*, 6, 337, DOI:10.3389/fmars.2019.00337, 2019.
1830
1831 TOURATIER Franck, POISSON Alain (1990) MINERVE, <https://doi.org/10.18142/128>
1832
1833 Touratier, F., and Goyet, C.: Decadal evolution of anthropogenic CO₂ in the north western Mediterranean Sea
1834 from the mid-1990's to the mid-2000's. Deep Sea Research Part I.doi:10.1016/j.dsr.2009.05.015, 2009.
1835
1836 Ulles, C., Estournel, C., Fourrier, M., Coppola, L., Kessouri, F., Lefèvre, D., and Marsaleix, P.: Oxygen budget
1837 of the north-western Mediterranean deep- convection region, Biogeosciences, 18, 937–960,
1838 <https://doi.org/10.5194/bg-18-937-2021>, 2021.
1839
1840 Ulles, C., Estournel, C., Marsaleix, P., Soetaert, K., Fourrier, M., Coppola, L., Lefèvre, D., Touratier, F., Goyet,
1841 C., Guglielmi, V., Kessouri, F., Testor, P., and Durrieu de Madron, X.: Seasonal dynamics and annual budget of
1842 dissolved inorganic carbon in the northwestern Mediterranean deep-convection region, Biogeosciences, 20,
1843 4683–4710, <https://doi.org/10.5194/bg-20-4683-2023>, 2023.
1844
1845 UNESCO: Intercomparison of total alkalinity and total inorganic carbon determinations in seawater. UNESCO
1846 Tech. Pap. Mar. Sci. 59., 1990
1847

- 1848 UNESCO: Reference materials for oceanic carbon dioxide measurements. UNESCO Tech. Pap. Mar. Sci. 60.,
 1849 1991
 1850
 1851 United Nations. The Sustainable Development Goals 2020, 68pp. <https://unstats.un.org/sdgs/report/2020/>., 2020
 1852
 1853 Vance, J. M., Currie, K., Suanda, S. H. and Law, C. S.: Drivers of seasonal to decadal mixed layer carbon cycle
 1854 variability in subantarctic water in the Munida Time Series. Front. Mar. Sci. 11:1309560. doi:
 1855 10.3389/fmars.2024.1309560, 2024
 1856
 1857 VERNEY Romaric, RABOUILLE Christophe (2012) MERMEX-ACCESS cruise, RV Téthys II,
 1858 <https://doi.org/10.17600/12450070>
 1859
 1860 VIVIER Frédéric, WAELBROECK Claire, MICHEL Elisabeth (2016) NEXT STEP,
 1861 <https://doi.org/10.18142/338>
 1862
 1863 VERNEY Romaric, RABOUILLE Christophe (2012) MERMEX-ACCESS cruise, RV Téthys II,
 1864 <https://doi.org/10.17600/12450070>
 1865
 1866 von Schuckmann, K., Minière, A., Gues, F., Cuesta-Valero, F. J., Kirchengast, G., Adusumilli, S., Straneo, F.,
 1867 Ablain, M., Allan, R. P., Barker, P. M., Beltrami, H., Blazquez, A., Boyer, T., Cheng, L., Church, J.,
 1868 Desbruyeres, D., Dolman, H., Domingues, C. M., García-García, A., Giglio, D., Gilson, J. E., Gorfer, M.,
 1869 Haimberger, L., Hakuba, M. Z., Hendricks, S., Hosoda, S., Johnson, G. C., Killick, R., King, B., Kolodziejczyk,
 1870 N., Korosov, A., Krinner, G., Kuusela, M., Landerer, F. W., Langer, M., Lavergne, T., Lawrence, I., Li, Y.,
 1871 Lyman, J., Marti, F., Marzeion, B., Mayer, M., MacDougall, A. H., McDougall, T., Monselesan, D. P., Nitzbon,
 1872 J., Otosaka, I., Peng, J., Purkey, S., Roemmich, D., Sato, K., Sato, K., Savita, A., Schweiger, A., Shepherd, A.,
 1873 Seneviratne, S. I., Simons, L., Slater, D. A., Slater, T., Steiner, A. K., Suga, T., Szekely, T., Thiery, W.,
 1874 Timmermans, M.-L., Vanderkelen, I., Wijffels, S. E., Wu, T., and Zemp, M.: Heat stored in the Earth system
 1875 1960–2020: where does the energy go?, Earth Syst. Sci. Data, 15, 1675–1709, <https://doi.org/10.5194/essd-15-1675-2023>, 2023.
 1876
 1877 Wagener, T., Metzl, N., Caffin, M., Fin, J., Helias Nunige, S., Lefevre, D., Lo Monaco, C., Rougier, G., and
 1878 Moutin, T.: Carbonate system distribution, anthropogenic carbon and acidification in the western tropical South
 1879 Pacific (OUTPACE 2015 transect), Biogeosciences, 15, 5221-5236, <https://doi.org/10.5194/bg-15-5221-2018>,
 1880 2018.
 1881
 1882 Wimart-Rousseau, C.: Dynamiques saisonnière et pluriannuelle du système des carbonates dans les eaux de
 1883 surface en mer Méditerranée, Sciences de l'environnement. Aix-Marseille Université, <https://hal.archives-ouvertes.fr/tel-03523187>, 2021
 1884
 1885 Wimart-Rousseau, C., Lajaunie-Salla, K., Marrec, P., Wagener, T., Raimbault, P., Lagadec, V., Lafont, M.,
 1886 Garcia, N., Diaz, F., Pinazo, C., Yohia, C., Garcia, F., Xueref-Remy,I., Blanc, P.-E., Armengaud, A., and
 1887 Lefèvre, D.: Temporal variability of the carbonate system and air-sea CO₂ exchanges in a Mediterranean human-
 1888 impacted coastal site. Estuarine, Coastal and Shelf Science. <https://doi.org/10.1016/j.ecss.2020.106641>, 2020.
 1889
 1890 Wimart-Rousseau, C., Wagener, T., Álvarez, M., Moutin, T., Fourrier, M., Coppola, L., Niclas-Chirurgien, L.,
 1891 Raimbault, P., D'Ortenzio, F., Durrieu de Madron, X., Taillandier, V., Dumas, F., Conan, P., Pujo-Pay, M. and
 1892 Lefèvre, D.: Seasonal and Interannual Variability of the CO₂ System in the Eastern Mediterranean Sea: A Case
 1893 Study in the North Western Levantine Basin. Front. Mar. Sci. 8:649246. doi: 10.3389/fmars.2021.649246, 2021
 1894
 1895 Wimart-Rousseau, C., Wagener, T., Bosse, A., Raimbault, P., Coppola, L., Fourrier, M., Ulses, C. and Lefèvre,
 1896 D.: Assessing seasonal and interannual changes in carbonate chemistry across two timeseries sites in the North
 1897 Western Mediterranean Sea. Front. Mar. Sci. 10:1281003. doi: 10.3389/fmars.2023.1281003, 2023.
 1898
 1899
 1900

- 1901 WMO/GCOS, 2018: <https://gcos.wmo.int/en/global-climate-indicators>, 2018
- 1902
- 1903 Yao, M. K., Marcou, O., Goyet, C., Guglielmi, V., Touratier, F., and Savy, J.-P.: Time variability of the north-
1904 western Mediterranean Sea pH over 1995-2011. Marine Environmental Research, doi:
1905 10.1016/j.marenvres.2016.02.016, 2016
- 1906
- 1907 Yoder, M. F., Palevsky, H. I., and Fogaren, K. E.: Net community production and inorganic carbon cycling in
1908 the central Irminger Sea. Journal of Geophysical Research: Oceans, 129, e2024JC021027.
1909 <https://doi.org/10.1029/2024JC021027>, 2024
- 1910
- 1911 Zhang, S., Wu, Y., Cai, W.-J., Cai, W., Feely, R. A., Wang, Z., et al. : Transport of anthropogenic carbon from
1912 the Antarctic shelf to deep Southern Ocean triggers acidification. Global Biogeochemical Cycles, 37,
1913 e2023GB007921. <https://doi.org/10.1029/2023GB007921>, 2023
- 1914